frontiers | Frontiers in Astronomy and Space Sciences

REVIEW
published: 13 June 2022
doi: 10.3389/fspas.2022.896245

Differentiating Between the Leading Processes for Electron Radiation Belt Acceleration

Solène Lejosne[1], Hayley J. Allison[2], Lauren W. Blum[3], Alexander Y. Drozdov[4], Michael D. Hartinger[5], Mary K. Hudson[6,7], Allison N. Jaynes[8], Louis Ozeke[9], Elias Roussos[10] and Hong Zhao[11]*

[1]Space Sciences Laboratory, University of California, Berkeley, Berkeley, CA, United States, [2]GFZ German Centre for Geosciences, Potsdam, Germany, [3]Laboratory for Atmospheric and Space Physics, University of Boulder, Boulder, CO, United States, [4]University of California, Los Angeles, Los Angeles, CA, United States, [5]Space Science Institute, Boulder, CO, United States, [6]Department of Physics and Astronomy, Dartmouth College, Hanover, NH, United States, [7]High Altitude Observatory, National Center for Atmospheric Research, Boulder, CO, United States, [8]Physics and Astronomy, University of Iowa, Iowa City, IA, United States, [9]Department of Physics, University of Alberta, Edmonton, AB, Canada, [10]Max Planck Institute for Solar System Research, Göttingen, Germany, [11]Department of Physics, Auburn University, Auburn, AL, United States

OPEN ACCESS

Edited by:
Misa Cowee,
Los Alamos National Laboratory (DOE), United States

Reviewed by:
Philip J. Erickson,
Massachusetts Institute of Technology, United States
Yoshiharu Omura,
Kyoto University, Japan
Qiugang Zong,
Peking University, China

***Correspondence:**
Solène Lejosne
solene@berkeley.edu

Specialty section:
This article was submitted to Space Physics, a section of the journal Frontiers in Astronomy and Space Sciences

Received: 14 March 2022
Accepted: 18 May 2022
Published: 13 June 2022

Citation:
Lejosne S, Allison HJ, Blum LW, Drozdov AY, Hartinger MD, Hudson MK, Jaynes AN, Ozeke L, Roussos E and Zhao H (2022) Differentiating Between the Leading Processes for Electron Radiation Belt Acceleration. Front. Astron. Space Sci. 9:896245. doi: 10.3389/fspas.2022.896245

Many spacecraft fly within or through a natural and variable particle accelerator powered by the coupling between the magnetosphere and the solar wind: the Earth's radiation belts. Determining the dominant pathways to plasma energization is a central challenge for radiation belt science and space weather alike. Inward radial transport from an external source was originally thought to be the most important acceleration process occurring in the radiation belts. Yet, when modeling relied on a radial diffusion equation including electron lifetimes, notable discrepancies in model-observation comparisons highlighted a need for improvement. Works by Professor Richard M. Thorne and others showed that energetic (hundreds of keV) electrons interacting with whistler-mode chorus waves could be efficiently accelerated to very high energies. The same principles were soon transposed to understand radiation belt dynamics at Jupiter and Saturn. These results led to a paradigm shift in our understanding of radiation belt acceleration, supported by observations of a growing peak in the radial profile of the phase space density for the most energetic electrons of the Earth's outer belt. Yet, quantifying the importance of local acceleration at the gyroscale, versus large-scale acceleration associated with radial transport, remains controversial due to various sources of uncertainty. The objective of this review is to provide context to understand the variety of challenges associated with differentiating between the two main radiation belt acceleration processes: radial transport and local acceleration. Challenges range from electron flux measurement analysis to radiation belt modeling based on a three-dimensional Fokker-Planck equation. We also provide recommendations to inform future research on radiation belt radial transport and local acceleration.

Keywords: radiation belts, Earth, giant planets, local acceleration, radial acceleration, chorus waves, ULF waves, diffusion

1 INTRODUCTION

The outer radiation belt of the Earth's magnetosphere contains a complicated balance of acceleration and loss processes. Previous studies have found that while some geomagnetic storms acted as a significant driver of energetic electron enhancements, others did not (Summers et al., 2004; Hudson et al., 2008). Studies of flux changes following geomagnetic storms reveal that the system is highly non-linear, with a wide range of driving inputs resulting in either enhancement or depletion events (Reeves et al., 2003; Baker et al., 2004). Multiple results have shown the importance of southward interplanetary magnetic field, IMF B_z, for driving electron enhancements (Blake et al., 1997; Li X. et al., 2011), although high-speed solar wind also contributes to the effect (Paulikas and Blake, 1979; Baker et al., 1997; Kanekal et al., 1999). The need to forecast and predict these events has spurred increasing interest in the mechanisms by which acceleration takes place in the outer radiation belt. High energy electrons have deleterious effects on spacecraft systems as they can penetrate through satellite walls and cause deep-dielectric charging (e.g., Baker et al., 1987, 2018; Horne et al., 2013). Findings and models established in the case of the Earth's radiation belts have been transposed to the outer planets, and in particular the giant planets, Jupiter, and Saturn, with the shared objective of furthering our understanding of the physics of a magnetosphere.

Determining the dominant pathways to plasma energization in the radiation belts usually means focusing on either 1) relatively slow, large-scale acceleration processes associated with radial transport or 2) localized acceleration processes occurring on relatively smaller spatiotemporal scales, i.e., local acceleration. The objective of this review is to provide tools to approach this dichotomy. The review was motivated by a joint panel discussion on "Radial Transport vs. Local Acceleration" in the radiation belts, that took place during the Geospace Environment Modeling (GEM) Virtual Summer Workshop in July 2021 (Drozdov et al., 2022). It exemplifies the profound impact of Professor Richard M. Thorne on radiation belt science (e.g., Horne and Tsurutani, 2019; Li W. and Hudson, 2019). It provides the necessary context to navigate the (still) controversial topic of electron radiation belt acceleration. It is organized as follows:

Section 2 provides observational and theoretical background. Specifically, the characteristics of MeV electron flux enhancements are summarized (**Section 2.1**). The most commonly discussed mechanisms for electron radiation belt acceleration are introduced (**Section 2.2**), together with the modeling framework used to quantify their effects (**Section 2.3**). In **Section 3**, we show how the picture for radiation belt acceleration evolved over the years in response to measurements from new missions, from an initial emphasis on radial diffusion (**Section 3.1**) to an emphasis on local wave-particle interactions (**Section 3.2**). We also provide a summary of the current state of the art at the outer planets (**Section 3.3**). The topic is summarized and further discussed in **Section 4**. In particular, we provide a synthesis of the challenges associated with differentiating between the leading processes for electron radiation belt acceleration (**Section 4.1**) and we present a few suggestions for future research directions (**Section 4.2**).

2 OBSERVATIONAL AND THEORETICAL BACKGROUND

Electron flux enhancements at MeV energies are viewed as signatures of radiation belt acceleration. The main characteristics of these electron flux enhancements are provided in **Section 2.1**. The two main mechanisms thought to drive radiation belt acceleration are introduced in **Section 2.2**. These processes are included in a radiation belt model, detailed in **Section 2.3**, in order to quantify, compare and contrast the overall effects of these two acceleration mechanisms on radiation belt dynamics.

2.1 Observations Motivating the Research on Electron Radiation Belt Acceleration

A significant component of energetic (up to 10 MeV) electrons is rapidly produced at times in the Earth's outer radiation belt, within a couple of days or less (e.g., Baker et al., 1994; Foster et al., 2014). **Figure 1** (from Baker et al., 2019) displays six years (September 2012–2018) of >1 MeV electron fluxes measured by the Relativistic Electron-Proton Telescope (REPT, Baker et al., 2021) onboard the Van Allen Probes (Fox and Burch, 2014), together with information on solar wind properties. It reveals the highly variable and energy-dependent nature of MeV electron dynamics in the outer radiation belt. Despite radiation belts being one of the first discoveries of the space age, numerous questions remain regarding the nature of the processes that can accelerate radiation belt electrons and produce the dynamics observed in **Figure 1**.

2.1.1 Characteristics of Electron Flux Enhancements in the Earth's Outer Belt

Electron fluxes routinely increase by several orders of magnitude within days in the Earth's outer radiation belt (**Figure 1**, the article by Reeves et al., 2013). This flux increase may or may not be preceded by a brief, large decrease (e.g., Blake et al., 1997). Broadly speaking, the radiation belt electron flux enhancements are coherent: Increases occur on similar timescales across the radiation belt energy spectrum (50 keV–10 MeV) and across the outer zone (equatorial radial distance, L, between ~3 Re and 6.5 Re), regardless of altitude (e.g., Kanekal et al., 2001). Yet, the specific characteristics of these enhancements are variable. **Figure 1** shows that the magnitude of MeV electron flux usually peaks at a variable location within the outer region (i.e., below geostationary orbit). The rise time for electron flux enhancements increases with energy (e.g., Blake et al., 1997). In addition, the frequency and the L-coverage for electron flux enhancements generally decrease with energy (e.g., Reeves et al., 2013; Zhao et al., 2016).

2.1.2 Association With Solar Activity and Solar Wind Properties

An association between the state of the Earth's outer belt and the Sun was established in the early days of radiation belt science

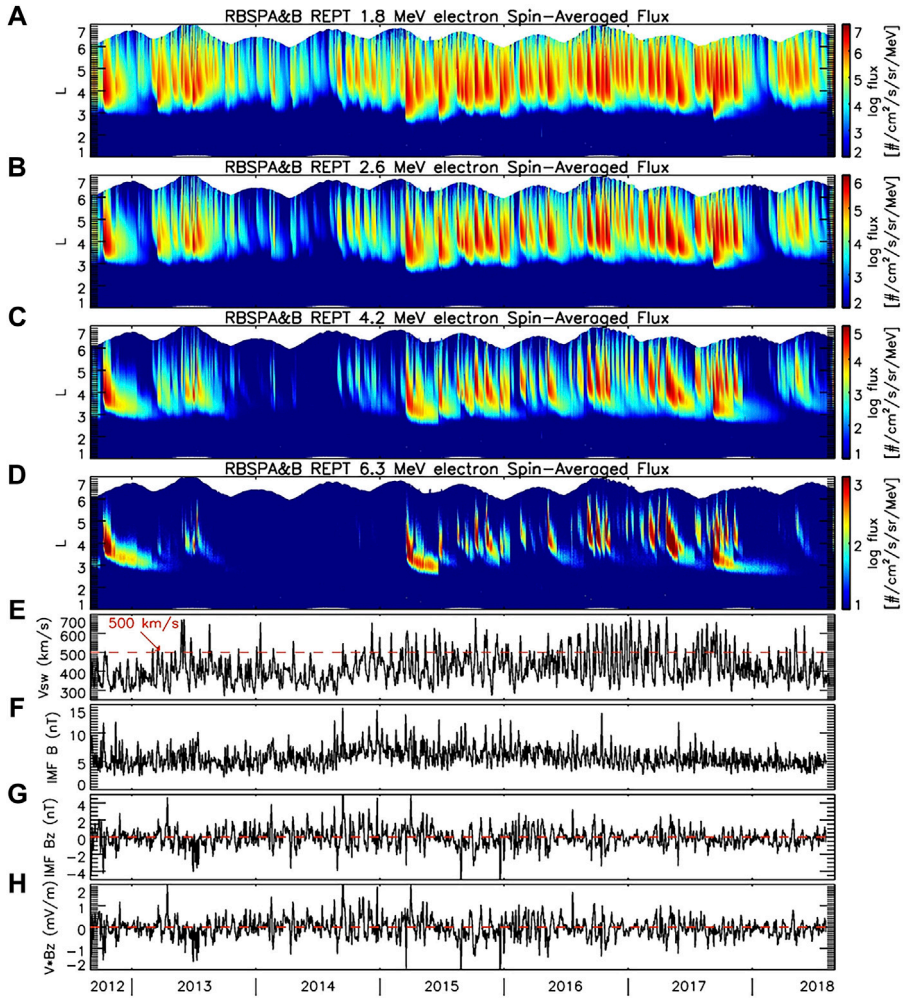

FIGURE 1 | Six years of MeV electron fluxes in the Earth's radiation belts, at **(A)** 1.8 MeV, **(B)** 2.6 MeV, **(C)** 4.2 MeV, and **(D)** 6.3 MeV, measured by both Van Allen Probes between 1 September 2012 and 1 September 2018, together with information on the solar wind properties, namely, the three-day running averages for **(E)** the solar wind speed, **(F)** the magnitude of the interplanetary magnetic field (IMF), **(G)** the north-south component of the IMF, Bz, and **(H)** the product of solar wind speed, V, and Bz (from Baker et al., 2019).

(Williams, 1966). It has remained a subject of research ever since (e.g., Hudson et al., 2008; Kellerman and Shprits, 2012; Kilpua et al., 2015; Zhao et al., 2019a; Ripoll et al., 2020). Connecting the Sun and solar wind properties with the state of the radiation belts is of prime importance for two main reasons. First, it provides observational constraints to radiation belt acceleration theories. Second, it constitutes the basis of radiation belt model developments, whether they are physics-based models (e.g., Xiang et al., 2021), empirical models such as AE9 and predecessors (Ginet et al., 2013), or machine learning models (e.g., Katsavrias et al., 2021a).

The most pronounced signature of the solar wind properties in the state of the Earth's outer radiation belt is the correlation between solar wind speed and MeV electron flux magnitude (Paulikas and Blake, 1979; Reeves et al., 2011; Wing et al., 2016). The sign of the north-south component of the interplanetary magnetic field (IMF), B_z, is also key (Blake et al., 1997). Most of the time, MeV electron flux enhancements occur when the speed of the solar wind is high ($\gtrsim$ 500 km/s) and the IMF B_z is southward, i.e., during conditions that are associated with geomagnetic storm times (e.g., Baker et al., 2019). While these solar wind conditions are the most common conditions for MeV electron flux enhancements, not all of them are necessary. Significant MeV electron flux enhancements have also been reported during non-storm times (e.g., Schiller et al., 2014) and without a high-speed solar wind (e.g., Li X. et al., 2011). A sustained southward IMF is the only necessary condition for MeV electron flux enhancements at geosynchronous orbit according to Li X. et al. (2011). Yet, this necessary condition is not a sufficient condition to guarantee radiation belt enhancements. Indeed, even though geomagnetic storms are associated with a strong and sustained southward IMF, not all geomagnetic storms result in electron flux enhancements (Reeves et al., 2003). The most significant relativistic electron flux enhancements occur outside the plasmapause, in association with periods of prolonged substorm

activity, as quantified by the AE index (Meredith et al., 2003). Moreover, MeV electron enhancements have been tied to High-Intensity Long-Duration Continuous AE Activity (HILDCAA) events (Tsurutani et al., 2006; Miyoshi and Kataoka, 2008; Hajra et al., 2015) and substorm clusters during geomagnetic disturbances (e.g., Rodger et al., 2022).

When electron flux enhancements occur during geomagnetic storms, the location of the peak in MeV electron flux enhancements during recovery phase is strongly correlated with the magnitude of the storm, as quantified by the Dst index (Tverskaya et al., 2003) or, equivalently, with the plasmapause location (O'Brien et al., 2003; Moya et al., 2017; Bruff et al., 2020). The equatorial pitch angle distribution of MeV electron flux enhancements at the center of the outer belt is most anisotropic (i.e., 90° peaked) within a day of the start of the recovery phase, and the degree of anisotropy increases with energy (e.g., Ozeke et al., 2022). The pitch-angle distribution of MeV electron flux becomes more isotropic in the week following the start of the recovery phase (Greeley et al., 2021).

One consequence of the relationship between the state of the Sun and the state of the Earth's outer radiation belt is that periodicities of the Sun, of the solar activity, and of the Sun-Earth connection lead to periodicities in the intensity of the outer belt occurring on a variety of timescales. For instance, the 27-day periodicity of the electron flux enhancements (Williams, 1966) is associated with the 27-day recurrence of geomagnetic activity. The latter comes from the fact that long-lived solar wind features, such as high-speed streams, recur at Earth after every Sun rotation period of ~27 days (e.g., Paulikas and Blake, 1979). The strong semiannual variations of MeV electron fluxes have been tied to the semiannual variation in the orientation between the Earth's magnetic dipole axis and the Sun vector, and more precisely, to the Russell-McPherron effect (McPherron et al., 2009; Katsavrias et al., 2021b). MeV electron fluxes are also more intense during the declining phase of the solar cycle than during the ascending phase. This is due to the fact that the declining phase of the solar cycle is dominated by recurrent high-speed solar wind streams while the ascending phase is dominated by more sporadic coronal mass ejection events (Kanekal, 2006; Reeves et al., 2011), and radiation belts respond differently to storms driven by coronal mass ejections (CMEs) and storms driven by corotating interaction regions (CIRs) (e.g., Turner et al., 2019).

2.2 Electron Radiation Belt Acceleration Mechanisms

Before relating observed electron flux enhancements (**Section 2.1**) to radiation belt energization (**Section 2.2.2**), we first provide a brief introduction to the theoretical framework associated with radiation belt dynamics (**Section 2.2.1**). While the concepts of adiabatic invariant theory are general, they are applied to the case of the Earth's radiation belts in the next paragraph.

2.2.1 Brief Introduction to Trapped Particles Dynamics and Adiabatic Invariant Theory

It takes a few hours down to a few minutes for the 50 keV to 5 MeV electrons of the outer belt to orbit around the Earth. During that time, these particles, trapped by the geomagnetic field, bounce 500 to 50,000 times from one hemisphere to the other while they gyrate 10^5 to 10^9 times around the magnetic field direction. In this context, it is convenient to describe the motion of radiation belt particles as the superposition of three quasi-periodic motions, each of them evolving on a very different timescale (e.g., Schulz and Lanzerotti, 1974):

1) A very fast motion of gyration around the magnetic field direction,
2) A slower bounce motion between the planet's hemispheres, and
3) A slow drift motion around the planet.

Each quasi-periodic motion is determined by the particle's characteristics (charge, mass, kinetic energy, pitch angle) as well as by the characteristics of the magnetic and electric fields (magnitude, direction, as well as spatial and temporal variability of the fields).

The magnitude of each quasi-periodic motion is quantified by an adiabatic coordinate, that is, by a quantity that is a constant of motion under certain spatial and temporal conditions. In particular, an adiabatic coordinate remains constant as long as the time variations for the fields are negligible on the timescale of the corresponding quasi-periodic motion (e.g., Northrop, 1963). That is why the reformulation of trapped particle dynamics in terms of adiabatic coordinates allows for a simplified description of radiation belt dynamics (e.g., Roederer, 2014).

In the absence of significant time variations in the fields, trapped radiation belt particles remain at about the same *average* equatorial radial distance from the center of the planet. They move along closed surfaces called *drift shells*. Their kinetic energy is conserved on average. In other words, in the steady state, there is neither net acceleration nor net deceleration occurring in the radiation belts. Energy variation for the trapped radiation belt particles requires time variations of the electric and/or magnetic fields. Since the magnetic force does no work, it is the electric field that exchanges energy with the trapped particles. This electric field may be induced by magnetic field time variations, or it may be due to variations in the electric potential. It is usually assumed that there is no component of the electric field parallel to the magnetic field direction, a good approximation in the inner magnetosphere on timescales longer than the gyro-period. In the DC realm, the electrical conductivity is orders of magnitude greater in the parallel direction of the magnetic field than in the perpendicular direction of the magnetic field so that the parallel conductivity is often approximated to be infinitely high (e.g., Stern, 1977).

2.2.2 Interpreting MeV Electron Flux Enhancements in Terms of Radiation Belt Acceleration

Electron flux enhancements are conventionally viewed as indicative of radiation belt acceleration because radiation belt spectra typically decrease with energy. Thus, the energization of a population of trapped particles is expected to manifest as a flux enhancement. The standard practice is to split the mechanisms driving radiation belt irreversible (i.e., non-adiabatic)

acceleration into two categories, depending on the source location of the population that is accelerated:

- The non-adiabatic acceleration is *local* when the energized population is already present within the drift shell.
- On the other hand, the non-adiabatic acceleration is *radial* (i.e., considered to be due to radial transport) when the energized population comes from another drift shell (i.e., roughly speaking, when the population was initially drifting at another average equatorial radial distance).

We focus below on the two most favored mechanisms for radiation belt energization, namely: 1) global acceleration *via* radial transport (**Section 2.2.2.1**) and 2) local acceleration *via* resonant interactions with chorus waves (**Section 2.2.2.2**). That said, many other mechanisms have been proposed over the years (see for instance the review by Friedel et al. (2002) for details).

2.2.2.1 Radial Acceleration and Radial Transport, Assuming Conservation of the First Two Adiabatic Anvariants

Acceleration by radial transport is usually associated with relatively slow field variations, occurring on a timescale longer than the bounce period. This includes ultra-low frequency (ULF) waves in the Pc4 and Pc5 ranges (2–22 mHz, (Jacobs, 1970)), which can be confined in magnetic local time (e.g., Li L. et al., 2017). One of the prevailing assumptions of radial transport mechanisms is that the first two adiabatic coordinates are conserved, as assumed below. That said, other types of radial transport processes have been proposed, and are expected to occur at times (e.g., Ukhorskiy et al., 2011; O'Brien, 2014).

In the following, we detail why acceleration is usually related to inward radial motion, and we illustrate the importance of analyzing radiation belt dynamics in terms of adiabatic coordinates.

2.2.2.1.1 Energization in a Dipole Field. In the special case of a dipole magnetic field, the association between inward radial transport and acceleration is straightforward. Drift shells are still in space, and they are conveniently labelled by their normalized equatorial radial distance, L (McIlwain, 1961). In that context, a particle transported from one drift shell to the other is displaced radially and its energy varies.

The relationship between radial transport and kinetic energy variation is straightforward when considering the conservation of the first two adiabatic invariants of the trapped particle. In the case of an equatorially trapped particle, we obtain that: $p^2/B = constant$, which is equivalent to: $p^2L^3 = constant$ in a dipole field, where $p = \sqrt{T\,(T + 2m_oc^2)}/c$ is the relativistic momentum, T is the kinetic energy, and B is the equatorial magnetic field strength. As a result, the amount of kinetic energy variation, dT, associated with the radial transport, dL, is defined as:

$$\frac{dT}{T} = -R\frac{(\gamma+1)}{\gamma}\frac{dL}{L} \tag{1}$$

where γ is the Lorentz factor and $R > 0$ is a function of pitch angle (e.g., Lejosne and Mozer, 2020, Eq. 9). The pitch-angle function is such that $R = 3/2$ for equatorial particles. It decreases monotonically with decreasing pitch angle, until reaching a minimum value of $R = 1$ for field-aligned particles. This means that, for the same amount of radial transport, dL, equatorial particles experience the greatest amount of kinetic energy variation, dT. In all cases, **Eq. 1** details why inward radial transport ($dL < 0$) is usually associated with trapped particle energization ($dT > 0$). It also shows that radial transport is energy dependent: For the same amount of kinetic energy variation, dT, the amount of relative radial transport, dL/L, decreases with increasing kinetic energy, T.

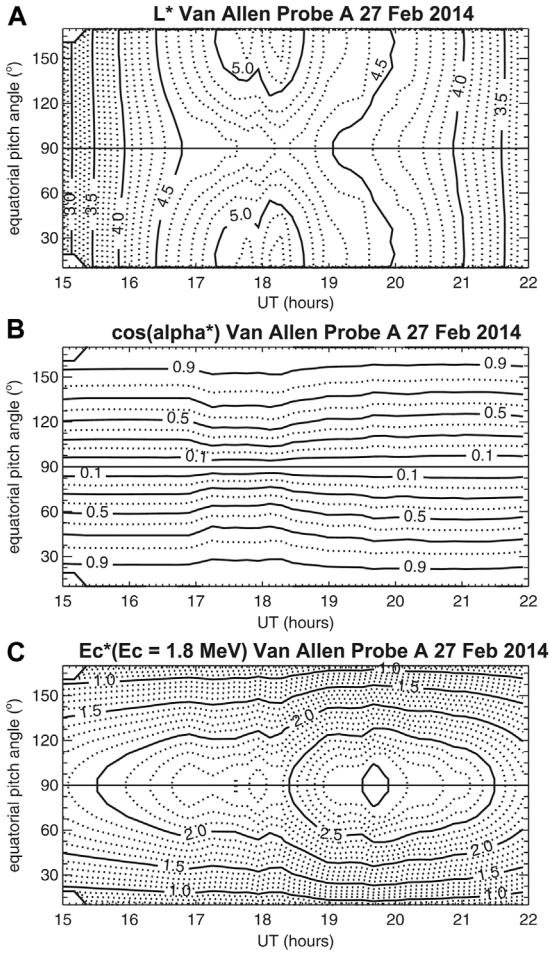

FIGURE 2 | The adiabatic coordinates $(L^*, \cos(\alpha^*), E_c^*)$ associated with a 1.8 MeV electron population measured by Van Allen probes A on the dayside during the 27 February 2014 event, as a function of the time of the measurement and for different equatorial pitch angles, α. From (Roederer and Lejosne, 2018).

2.2.2.1.2 Energization in a Distorted Field. At times, especially during active times in the Earth's outer belt, the magnetic field significantly departs from the dipole assumption. In that case, the relationship between inward radial transport and acceleration is more complex than **Eq. 1**. There is no longer a one-to-one correspondence between drift shell and normalized average

equatorial radial distance. The conservation of the first two adiabatic invariants only relates an amount of kinetic energy variation to an amount of magnetic field variation. Thus, an amount of kinetic energy variation does not inform about the amount of radial transport or change of drift shell for the trapped population. In the case of an equatorial particle, the relationship with kinetic energy variation, dT, and equatorial magnetic field variation, dB, is:

$$\frac{dT}{T} = \frac{1}{2}\frac{(\gamma+1)}{\gamma}\frac{dB}{B} \tag{2}$$

Trapped particles gain energy as they experience regions of higher magnetic field magnitude. Yet, this relationship does not tell us if particles travel from one drift shell to the other, or not. In other words, it does not inform us on the variation of the third adiabatic invariant. In fact, a population can gain kinetic energy and move radially in space while remaining on the same drift shell (i.e., while all three adiabatic invariants remain constant). Hence, "energization by radial motion" does not necessarily mean "violation of the third adiabatic invariant", because inward or outward radial motion can be fully adiabatic (see also, Lejosne and Kollmann, 2020). Such consideration demonstrates the importance of carefully defining the terms used to describe radiation belt acceleration.

To further illustrate this idea, **Figure 2** provides the (L^*, α^*, E_c^*) adiabatic coordinates associated with a population of 1.8 MeV electrons measured by Van Allen Probes A during the geomagnetic storm of 27 February 2014 (e.g., Xiang et al., 2017). The (L^*, α^*, E_c^*) coordinates were introduced by Roederer and Lejosne (2018) to provide a more intuitive quantification of the more commonly used adiabatic coordinates. They correspond to the equatorial radius of the drift shell (L^*), to the equatorial pitch angle (α^*), and to the kinetic energy (E_c^*) that the trapped 1.8 MeV electrons would have if the distorted magnetic field *slowly* turned into a dipole field (i.e., on a timescale that is slow enough to guarantee conservation of all three adiabatic coordinates). In the case of **Figure 2**, the quantities were computed assuming that the magnetic field is described by the model of Tsyganenko and Sitnov (2005). The spacecraft location and magnetic activity indices required by the magnetic field model were updated every 5 min. There is a small pocket of 1.8 MeV near-equatorial electrons with $E_c^* > 3$ MeV at $L^* \sim 4.4$ measured by Van Allen probes A around 19:40 UT, when the spacecraft is at $L = 5.5$. This means that, if no other processes occurred besides a *slow* magnetic field dipolarization (i.e., occurring on a timescale slower than their 10-min drift period), these trapped particles would be transported inward, from their current location in the compressed magnetic field, at $L = 5.5$, down to an equatorial altitude of 4.4 Earth radii, moving inward by 1.1 Earth radii while maintaining all three adiabatic coordinates constant (including $L^* = constant \sim 4.4$). They would become >3 MeV electrons: a >1.2 MeV energy gain that represents more than 65% of their initial kinetic energy. This amount of kinetic energy variation is altered by non-adiabatic effects that occur when field variations take place on a shorter timescale (<10 min). In short, it is important to take into account fully adiabatic processes when discussing trapped particle acceleration during active times in the Earth's outer belt (see also, Dessler and Karplus 1961; Kim and Chan 1997).

During data analysis, the component of radiation belt energization that is due to fully adiabatic processes (i.e., processes conserving all three adiabatic invariants) is the first component to be isolated by converting flux measurements into phase space density (PSD) parameterized in terms of adiabatic coordinates. The remaining dynamics result from processes that violate at least one adiabatic coordinate. **Figure 3**, from Jaynes et al. (2018), illustrates how mapping measured fluxes into adiabatic space provides a significantly different picture of radiation belt dynamics.

In this context, the correlation between the state of the Earth's outer belt and solar wind properties, as well as geomagnetic activity (**Section 2.1.2**) was revisited and quantified in terms of electron PSD and PSD dynamics (Zhao et al., 2017). In particular, electron PSD enhancements were shown to correlate well with the AL index, strengthening the role played by substorms in radiation belt acceleration.

2.2.2.1.3 Radial Transport, From One Drift Shell to Another. Defining radial transport as a motion from one drift shell to another, i.e., from one L^* coordinate to the other, allows us to disentangle adiabatic from non-adiabatic energization processes. The motion of a trapped particle from one drift shell to the other is associated with a violation (i.e., time variation) of its third adiabatic coordinate. The violation of a population's third adiabatic coordinate requires that 1) the time variations of the field occur on a timescale that is relatively short with respect to the drift period, and that 2) the time variations are asymmetric, i.e., that they vary with magnetic local time (e.g., Northrop, 1963). A detailed discussion of this process is provided in the review by Lejosne and Kollmann (2020), together with a derivation of the expression for the instantaneous rate of change of L^*.

When discussing radial transport from one drift shell to the other in the context of radiation belt acceleration, the focus is on two main regimes:

1) A coherent, sudden and significant variation of the third adiabatic coordinate, as in the case of a shock-induced acceleration associated with an injection or a drift resonant interaction, with an immediately significant effect on trapped particle dynamics (Li X. et al., 1993; Zong et al., 2009; Schiller et al., 2016; Hudson et al., 2017; Hao et al., 2019), or;
2) Many small uncorrelated variations in L^*, with a cumulative effect that becomes progressively significant for the trapped particle dynamics. This effect is conventionally assumed to be diffusive on sufficiently long timescales (e.g., Ukhorskiy and Sitnov, 2012). The magnitude of this radial diffusion process, i.e., the diffusion coefficient, D_{LL}, is defined as:

$$D_{LL} = \frac{\left[(\Delta L^*)^2\right]}{2\Delta t} \tag{3}$$

where the operator [ ] is the average over all magnetic local time sectors, and over many events (i.e., over many drift periods), and

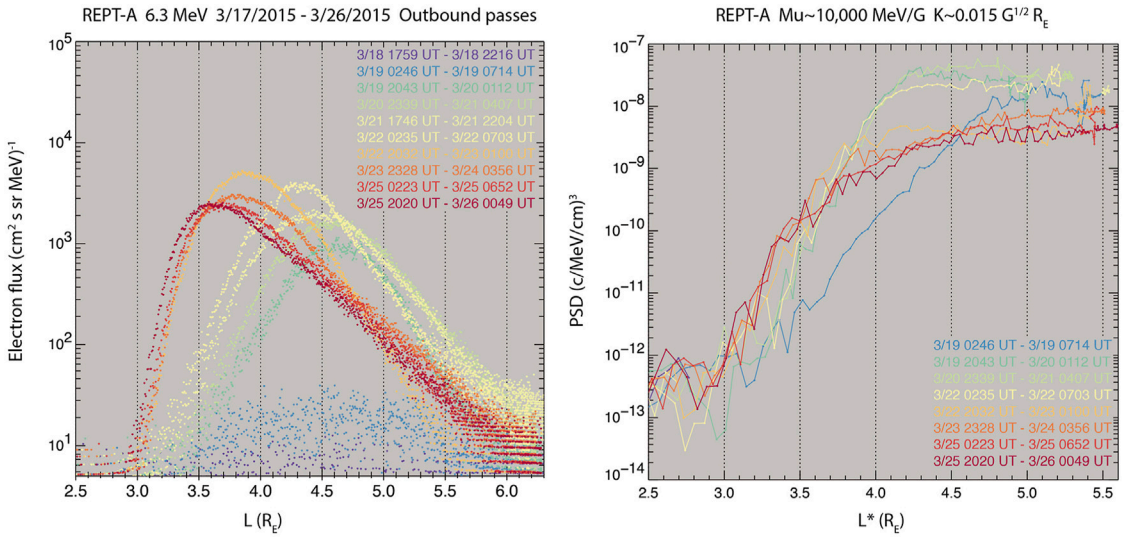

FIGURE 3 | (left) Time evolution of the 6.3 MeV electron flux as a function of the normalized equatorial radial distance, L, from 17 March 2015 to 26 March 2015; (right) Time evolution of the phase space density (PSD) of near equatorial electrons as a function of the L^* coordinate (for a first adiabatic invariant set to 10,000 MeV/G). From Jaynes et al. (2018).

ΔL^* corresponds to the total variation in L^* after a time interval, Δt. In theory, $[(\Delta L^*)^2]$ grows linearly with time once the time interval Δt is greater than the autocorrelation time for the variations of the field. As a result, D_{LL} is independent of the choice of Δt under this regime of normal diffusion.

These two regimes correspond to 1) non-linear and 2) quasi-linear descriptions of the large-scale wave-particle interactions.

Regardless of the type of radial transport process considered (fully adiabatic radial motion, rapid transport from one drift shell to the other, or slow diffusion from drift shell to drift shell), the amount of energy variation remains constrained by the conservation of at least the first two adiabatic coordinates. In the 1990s, it was suggested that fluxes of 20–200 keV electrons in the solar wind were insufficient to account for fluxes of MeV electrons measured in the Earth's outer belt, assuming that these electrons were simply transported radially inward (e.g., Li X. et al., 1997). While this finding was later questioned (e.g., Turner et al., 2021), it highlighted the need for an additional acceleration process at the time, and local acceleration by chorus waves was brought forward (e.g., Thorne, 2010).

2.2.2.2 Local Acceleration Associated With the Violation of the First Adiabatic Invariant

The other dominant mechanism for the acceleration of energetic (≳100 keV) electrons is resonant interactions with very low frequency (VLF) whistler-mode chorus waves outside the plasmasphere (e.g., Horne and Thorne, 1998; Summers et al., 1998; see also the reviews by: Bortnik et al., 2016; Koskinen and Kilpua, 2022). Chorus waves are naturally occurring electromagnetic emissions, commonly found in the Earth's radiation belt region. Plasma sheet electrons supplied to the inner magnetosphere during geomagnetically active times are unstable to the generation of whistler-mode chorus waves (e.g., Kennel and Thorne, 1967). The chorus emissions grow from thermal noise with a linear rate driven by the anisotropic distribution of these injected electrons, whose perpendicular temperature is greater than their parallel temperature (Kennel and Petschek, 1967). The path-integrated gain is sufficient to raise wave amplitudes to nonlinear levels (Li W. et al., 2007) where nonlinear trapping of electrons takes place (Nunn et al., 2003). Omura and Summers (2004) showed that chorus waves then ultimately grow non-linearly to a saturation level. As chorus waves propagate, they can interact resonantly with energetic electrons.

A resonance occurs when the Doppler-shifted wave frequency matches a multiple of the cyclotron frequency of an energetic electron moving through the wave packet, i.e., when:

$$\omega - k_{\parallel} v_{\parallel} = \frac{n\Omega_{ce}}{\gamma} \tag{4}$$

where ω is the frequency of a single wave, n is an integer ($n = 0, \pm 1, \pm 2, \ldots$), Ω_{ce}/γ is the magnitude of the electron gyrofrequency retaining the sign of the electron charge, k is the wave vector, and v is the electron velocity, where the parallel suffix indicates the direction parallel to the background magnetic field. The case of $n = 0$ corresponds to the Landau resonance where $\omega = k_{\parallel} v_{\parallel}$, and can arise when the chorus waves have an electric field component parallel to the background magnetic field, i.e., a non-zero wave normal angle. The cases $n = \pm 1, \pm 2, \ldots$ correspond to Doppler shifted cyclotron resonances. Here, in the frame of reference of the electron moving along the magnetic field, the wave frequency is Doppler shifted to the electron's cyclotron frequency and the electron experiences an electric field rotating at n times its rate of gyration. The electron is then accelerated or decelerated by this

electric field depending on the phase of the wave in relation to the electron's gyration phase. Whistler waves have frequencies below the electron cyclotron frequency, and so, in the case of a chorus wave propagating along the magnetic field, the frequency must be Doppler shifted up in order to achieve an $n = -1$ resonance with electrons. In the case of relativistic particles, where $\gamma > 1$, a smaller upwards Doppler shift is necessary for resonance than in the case of non-relativistic particles. The negative sign on the left-hand side of **Eq. 4** then needs to become positive, which can be achieved when $k_\parallel$ and $v_\parallel$ have different signs and, therefore, the waves resonate with electrons traveling in the opposite direction. Resonances where $|n| > 1$ take place for obliquely propagating waves as the wave field is then elliptically polarized, constructed from left- and right-handed wave components. In the non-relativistic case, $\gamma = 1$, and we can solve **Eq. 4** to obtain the parallel velocity of an electron in Doppler-shifted cyclotron resonance with the wave. As relativistic effects become important, the perpendicular component of the electron velocity, $v_\perp$, is introduced to the resonance condition *via* γ and a semi-ellipse in $v_\parallel$ and $v_\perp$ space defines the resonant velocities, constraining the resonant electron energies.

In case of resonance, the wave phase velocity, $\omega/k_\parallel$, and the components of the particle's velocity perpendicular and parallel to the ambient magnetic field, $v_\perp$ and $v_\parallel$, respectively, become linked. This relationship allows for efficient energy exchange between the wave and the electron. Gendrin (1981) showed that, for small amplitude waves, the kinetic energy of the electron is conserved in the reference frame of the wave. Transforming back to the lab reference frame in the non-relativistic case:

$$\left(\frac{\omega}{k_\parallel} - v_\parallel\right)^2 + v_\perp^2 = constant \tag{5}$$

and the electron can gain or lose energy to the monochromatic wave, potentially changing both the pitch angle and energy of the electron. For the interested reader, the relativistic case is shown by Summers et al. (1998). As $v_\parallel$ (and for the relativistic case $v_\perp$) changes, the phase velocity, and therefore the frequency of the wave that the electron resonantly interacts with, also changes in accordance with the resonance condition.

In practice, chorus waves are not monochromatic, i.e., they have a band width. For each wave frequency, **Eq. 5** defines a circle (or in the relativistic case, an ellipse) in $v_\parallel$ and $v_\perp$ space known as a *single wave characteristic*. The single wave characteristics cross the resonance condition in velocity space. Thus, a diffusion curve is defined in $v_\parallel$ and $v_\perp$, every point of which is tangential to some single wave characteristic, corresponding to a particular wave frequency. As mentioned above, electrons in Doppler-shifted cyclotron resonance can be accelerated or decelerated by the chorus wave according to the angle between the wave's magnetic field and the instantaneous perpendicular velocity of the electron. As such, electrons move randomly up or down single wave characteristics and the net behavior is in the direction of the decreasing particle distribution function along the single wave characteristic. A series of resonant interactions with chorus waves covering a range of frequencies then results in a net change of the particle's energy and pitch angle. The usual assumption is that each wave-particle interaction results in a small perturbation of the particles' characteristics. In that case, the cumulative effect of many interactions between chorus waves and radiation belt electrons is diffusive in energy and pitch angle.

When introducing more realistic conditions, including large amplitude waves, significant variations in energy and pitch angle can occur during a single interaction, and non-linear behaviors need to be considered (e.g., Bortnik et al., 2016). Theoretical analysis and test particle simulations have enabled detailed descriptions of the microphysics of chorus wave-particle interactions (e.g., Omura, 2021). They have shown how energetic electrons phase-trapped in coherent whistler waves can gain significant amount of energy over very short timescales (e.g. Albert, 2002). In particular, they have highlighted effective electron energization mechanisms, such as the relativistic turning acceleration of radiation belt electrons by chorus waves of sufficiently large amplitude (Omura et al., 2007), combined with ultra-relativistic acceleration interactions (Summers and Omura, 2007; Omura et al., 2015). Effective acceleration can occur through successive nonlinear trappings by consecutive multiple sub packets of a chorus wave element (Hiraga and Omura, 2020).

As a result, there is a dichotomy similar to what exists for radial transport modeling when it comes to describing local acceleration associated with the violation of the first adiabatic invariant in the radiation belts:

1) A non-linear framework, which can detail coherent, sudden and significant variations of the trapped electrons' energy and pitch angle *via* phase-trapping with realistic chorus wave models, and;
2) A quasi-linear model, where many small uncorrelated variations in pitch angle and energy have a cumulative effect that becomes progressively significant for the trapped particle dynamics, and that is assumed to be diffusive on sufficiently long timescales.

2.3 Modeling Framework to Quantify and Compare the Effects of Local and Radial Acceleration on Radiation Belt Dynamics

In order to quantify the effects of local and radial acceleration, and to put them into context, it is necessary to choose a global framework in which to model radiation belt dynamics. Here, it is important to realize that modeling implies trading off accuracy against practicality. A limit to the level of accuracy achievable by a radiation belt model is a potential limit to the level of accuracy with which the effects of local and radial acceleration can be quantified. Thus, it is important to keep in mind the set of assumptions underlying a radiation belt model and to remember the scope of the modeling framework. The formalism adopted by most radiation belt models (**Section 2.3.1**) as well as the limits to its accuracy (**Section 2.3.2**) are summarized below.

2.3.1 The Fokker-Planck Formalism, a Convenient Approximation for Radiation Belt Models

A detailed and accurate modeling of radiation belt particle dynamics is nothing short of impossible: It would require a

complete and highly accurate specification of the spatial and temporal variations of the electromagnetic fields on a multiplicity of spatio-temporal scales—from the drift-scale down to the gyro-scale. Particle-in-cell simulations allow for self-consistent interactions between particles and wave fields to be simulated, however computational requirements are high and only small spatial scales and time periods can be modelled this way (e.g., Camporeale, 2015; Allanson et al., 2019). Even when the fields are specified by numerical models (e.g., MHD fields), injecting test particles to simulate radiation belt dynamics remains cumbersome. This impossibility calls for necessary tradeoffs. A powerful way to reduce the number of variables to handle is the use of the adiabatic theory of magnetically trapped particles (**Section 2.2.1**). Adiabatic theory *"provides correct answers only as long as we don't look too close and are not expecting too detailed information"* (Roederer and Zhang, 2014). To account for uncertainties in electromagnetic field dynamics, we leverage probability theory, in particular the Fokker-Planck formalism. This formalism accounts for uncertainty by assuming random changes in the variables, relating average characteristics of the electromagnetic fields to average properties of the radiation belt dynamics. It is these tools (Fokker-Planck equation and adiabatic invariant theory) that have been successfully combined for more than 25 years (Beutier and Boscher, 1995) to facilitate operational radiation belt modeling. In particular, these simplifications allow for radiation belt simulations over long time intervals (months to years) (e.g., Glauert et al., 2018).

Specifically, most physics-based radiation belt models consist of solving a Fokker-Planck equation reduced to a diffusion equation, with the objective of providing an approximate description for the time evolution of the radiation belts:

$$\frac{\partial f}{\partial t} = \sum_{i,j} \frac{\partial}{\partial J_i}\left(D_{i,j} \frac{\partial f}{\partial J_j} \right) + Sources - Losses \qquad (6)$$

where $f(J_1, J_2, J_3)$ is the *drift-averaged* particle distribution function, J_i are the action variables, proportional to the adiabatic coordinates, and $D_{i,j}$ are the *drift-averaged* diffusion coefficients (e.g., Schulz and Lanzerotti, 1974). The "*Sources*" and "*Losses*" terms account for other non-diffusive processes affecting the distribution function. In practice, diffusion in terms of action variables is often reformulated in different coordinate systems. In particular, diffusion in terms of pitch angle, energy and L^* is often preferred. Thus, diverse reformulations of the same **Eq. 6** exist.

Defining realistic boundary conditions and performing model-observation comparisons require relating the variables of **Eq. 6** to measurable quantities. On one hand, it is straightforward to relate the trapped particle distribution in phase space (i.e., the phase space density, PSD) to experimental data: PSD is proportional to the directional differential flux, a measurable quantity (e.g., Roederer, 1970, p.93). On the other hand, defining the adiabatic coordinates cannot be done relying solely on experimental data. Indeed, since the adiabatic coordinates are:

1) $\mu = p_\perp^2 / 2 m_o B$, where m_o is the particle rest mass.

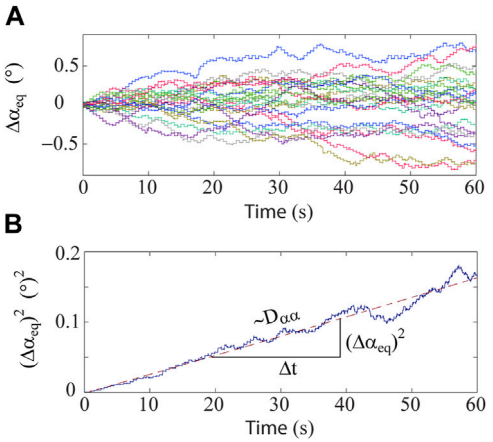

FIGURE 4 | A long-run simulation of 24 electrons experiencing cumulative linear scattering interactions, resulting in quasilinear diffusive behavior. **(A)** Change in equatorial pitch angle of all particles as a function of time. **(B)** The variance of all particles equatorial pitch angles increases linearly as a function of time, consistent with diffusive scattering. The rate of change of the variance yields the pitch angle diffusion coefficient, $D_{\alpha\alpha}$. Adapted from Bortnik et al. (2016).

2) $J = \oint p_\parallel ds$, where the integral goes over the full bounce motion along the magnetic field line, and
3) $\Phi = \oint_\Gamma \boldsymbol{A} \cdot \boldsymbol{dl} \propto 1/L^*$, where $\boldsymbol{A}$ is the magnetic potential vector and Γ is the instantaneous drift contour delimiting the drift shell,

Quantifying the adiabatic coordinates of MeV populations associated with a PSD sample requires information on the instantaneous magnetic field topology along the full drift contour. This means working with a magnetic field model. In addition, the adiabatic coordinates of a measurement can be undefined under certain conditions, as in the case in the presence of open drift shells—where particles are lost before completing a full drift around the Earth. This is a spatial limit to the scope of the model and outer boundary specification (e.g., Albert et al., 2018).

2.3.2 Limits to the Diffusion-Driven Radiation Belt Model

Diffusion-driven radiation belt models solving **Eq. 6** are thought to work best for very high energy particles (e.g., Fok, 2020). That said, they remain limited in several ways, as discussed below.

First, **Eq. 6** assumes that radiation belt dynamics are mainly due to physical processes whose overall effects can be encapsulated by diffusion coefficients. In other words, according to **Eq. 6**, radiation belt dynamics are primarily due to many very small, uncorrelated, time-stationary field fluctuations, resulting in many very small ($\Delta J_i / J_i \ll 1$), uncorrelated, perturbations of the trapped particle dynamics, akin to random walks in phase space at all scales—from the drift-scale down to the gyro-scale. In this diffusive picture, the scattering of a population of particles with the same initial characteristics increases linearly with time in phase space. This concept is illustrated in **Figure 4** in the case of pitch angle diffusion.

The postulate of a regime that is mainly diffusive also means that **Eq. 6** is ill-suited at times when particle dynamics are coherent, in particular at times when significant particle injections occur, and at times when large amplitude waves result in non-diffusive regimes (e.g., nonlinear phase bunching, phase trapping) (e.g., Riley and Wolf, 1992; Albert, 2002; Bortnik et al., 2008; Ukhorskiy et al., 2009; Omura et al., 2015).

Second, **Eq. 6** cannot resolve radiation belt dynamics on a timescale shorter than that of drift phase mixing. The dynamics of the PSD described by **Eq. 6** are drift-averaged. As a result, all equation variables are independent of magnetic local time by design. This means, for instance, that radiation belt drift echoes (e.g., Lanzerotti et al., 1967) cannot be reproduced using **Eq. 6**. That is also why this framework cannot reproduce shock-injections during sudden storm commencements for instance. In this case, the modelling efforts favor test particle simulations (e.g., Li X. et al., 1993; Hudson et al., 1997: Kress et al., 2007: Hudson et al., 2017).

3 ACCELERATION IN THE RADIATION BELTS: AN EVOLVING PICTURE

Keeping the observational (**Section 2.1**) and theoretical (**Sections 2.2**, **2.3**) context in mind, this section describes how the picture of radiation belt acceleration has evolved over the past 25 years, from an emphasis on radial diffusion (**Section 3.1.1**) to a paradigm shift underscoring the role of local acceleration in the radiation belts (**Section 3.1.2**). At the outer planets, a consensus is still pending, as detailed in **Section 3.2**. Unambiguously solving this puzzle remains a challenge, discussed in **Section 3.3**.

3.1 From the Importance of Radial Diffusion to the Importance of Local Wave Particle Interactions in the Earth's Radiation Belts

Radial diffusion from an external source towards the planet was originally thought to be the main mechanism for radiation belt acceleration (e.g., Fälthammar, 1965). When modeling relied on a radial diffusion equation including electron lifetimes, shortcomings in model-data comparisons highlighted a need for improvement. As a result, the role of local acceleration was brought forward (e.g., Horne and Thorne, 1998; Green and Kivelson, 2004; Horne et al., 2005; Koller et al., 2007; Reeves et al., 2013). This was supported in particular by observations of a growing peak in the radial PSD profile of the most energetic electrons of the Earth's outer belt, derived from measurements made during the recovery phase of geomagnetic storms (e.g., Brautigam and Albert, 2000; Iles et al., 2006). These points are detailed in this **Section 3.1**.

3.1.1 From Radiation Belt Modeling Based on the Normal Diffusion Equation

A first version of **Eq. 6** focuses on the effects of 1) radial diffusion and 2) losses due to pitch angle scattering into the loss cone, meaning finite electron lifetimes:

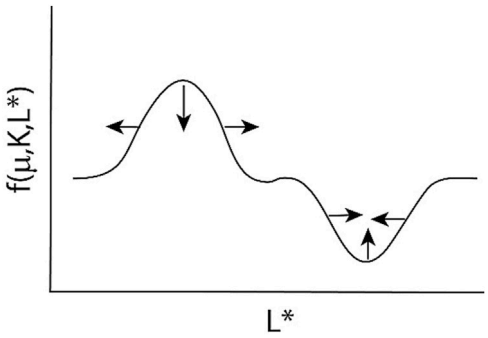

FIGURE 5 | Time evolution of a PSD described by a normal radial diffusion equation (from Green and Kivelson, 2004).

$$\frac{\partial f}{\partial t} = L^2 \frac{\partial}{\partial L}\left(\frac{D_{LL}}{L^2}\frac{\partial f}{\partial L}\right) - \frac{f}{\tau} \tag{7}$$

where L stands for L^*, inversely proportional to the third adiabatic coordinate, D_{LL} is the radial diffusion coefficient, and τ is the electron lifetime resulting from the combined effect of the pitch angle scattering induced by different waves.

The use of the master **Eq. 7** to describe radiation belt dynamics constrains the range of possible time variations for the modeled PSD. Indeed, following Fick's first law of diffusion, the net "current" of particles that flow through a unit area of drift shell per unit of time, i.e., the diffusion flux, is (e.g., Walt, 1994):

$$\text{"Current"} = -\frac{D_{LL}}{L^2}\frac{\partial f}{\partial L} \tag{8}$$

This means that radial diffusion acts to smooth the PSD radial profile. In other words, radial diffusion decreases peaks and increases valleys present in the PSD radial profile. An illustration is provided in **Figure 5**, in the case of a 1D diffusion equation in the absence of loss.

D_{LL} contains all the information on the physical processes that drive cross drift shell motion, i.e., it quantifies the *efficiency* of the radial diffusion process, and it directly relates to the field dynamics. Yet, the magnitude of D_{LL} alone is not enough to determine how much radial diffusion affects radiation belt dynamics. Indeed, it is the *"Current"* quantity, i.e., $-(D_{LL}/L^2)(\partial f/\partial L)$ (**Eq. 8**), that determines the *manifestation* of the diffusion process – that is, it is this quantity that drives the PSD time variations, $\partial f/\partial t$ (**Eq. 7**). Thus, if the PSD radial gradient, $\partial f/\partial L$, is significant, the effect of radial diffusion may appear significant, even if the magnitude of the radial diffusion coefficient D_{LL} is relatively small (as is the case at very low L shells in the Earth's inner radiation belt for instance). Conversely, if the PSD radial gradient is relatively small, radial diffusion may appear unimportant for the dynamics of this region of the belts, regardless of the magnitude of the radial diffusion coefficient. This reasoning applies to all diffusion modes. It demonstrates the importance of taking into account PSD gradients when comparing the effects of various diffusion processes (i.e., various waves) on the time

evolution of the PSD. This also highlights the difficulty of directly relating measured wave power to PSD and/or flux variations (e.g., Simms et al., 2021).

Solving **Eq. 7** for the PSD, f, requires characterizing the radial diffusion coefficient, D_{LL}, the electron lifetime, τ, and setting boundary conditions. Different studies choose different settings. The time-varying coefficients, D_{LL}, are often provided by an empirical law for electromagnetic radial diffusion, such as defined by Brautigam and Albert (2000) for example based on a combination of *in situ* and ground-based measurements of time-varying magnetic fields parametrized by a geomagnetic activity index (Kp). More recent data sets have used both ground-based and *in situ* magnetic and electric field measurements to infer D_{LL} (Ozeke et al., 2014a; Liu et al., 2016; Ali et al., 2016; Sandhu et al., 2021). Radial diffusion coefficients can also be determined from solar wind measurements (e.g., Li X. et al., 2001; Lejosne, 2020) or MHD test-particle simulations (Tu et al., 2012; Li Z. et al., 2017). The electron lifetime is usually parameterized based on plasmapause location and magnetic activity (e.g., Orlova et al., 2016). In all cases, the solution of the standard diffusion equation (**Eq. 7**) displays much of the variability of the Earth's outer belt on long timescales (months to years) (e.g., Li X. et al., 2001; Shprits et al., 2005; Chu et al., 2010; Ozeke et al., 2014b; Drozdov et al., 2015, 2017). In particular, it describes radiation belt dynamics well during geomagnetically quiet times (e.g., Selesnick et al., 1997; Su et al., 2015; Ripoll et al., 2019).

However, model-observation comparisons can also present notable discrepancies, in particular for MeV electron fluxes during the recovery phase of magnetic storms (e.g., Brautigam and Albert, 2000; Shprits et al., 2005; Shprits et al., 2007a; Ozeke et al., 2020). Specifically, the development of a peak in the PSD radial profile of the outer belt has been put forward as evidence of the effect of an additional local acceleration mechanism (e.g., Miyoshi et al., 2003; Chen et al., 2007; Reeves et al., 2013): It is contrary to what is expected from radiation belt dynamics driven primarily by radial diffusion (**Figure 5**). A growing local peak in the PSD radial profile appears to be a common feature of PSD enhancement events—at least for near-equatorial particles with a first adiabatic coordinate that corresponds to ~1 MeV at L = 5. Indeed, based on four years of flux measurements from Time History and Events of Macroscale Interactions during Substorms (THEMIS) and Van Allen Probes converted into PSD, 70 out of 80 observed enhancement events presented a growing peak (Boyd et al., 2018). The geomagnetic conditions for a growing peak are variable: 38 out of 70 occurred during moderate or strong storms, while 32 occurred during small storm or non-storm times (i.e., with a Dst index no less than −50 nT). In all cases, the location of the local peak in the PSD radial profile was shown to be outside of the plasmasphere, about 1.25 Earth radius away from the plasmapause location on average.

3.1.2 To the Current State of the Art

When the effect of chorus waves on radiation belt dynamics is included as an additional source term in the Fokker-Planck equation (e.g., Tu et al., 2009; Xiang et al., 2021), or, more commonly as additional diffusion terms (e.g., Varotsou et al., 2005; Glauert et al., 2018), the quality of radiation belt modeling improves: Simulations yield a peak in the PSD radial profile, in reasonable agreement with observations (e.g., Shprits et al., 2008; Subbotin et al., 2010; Thorne et al., 2013; Ma et al., 2018; Wang and Shprits, 2019).

This apparent improvement in radiation belt modeling leads to the "two-step" picture for the acceleration to relativistic and ultra-relativistic energies in the outer radiation belt, in which both local and radial processes contribute to MeV electron production. This mechanism is well supported by both case studies (e.g., Jaynes et al., 2015; Zhao et al., 2018) and statistical analysis (e.g., Zhao et al., 2019b). It works as follows: First, the injection of source (tens of keV) and seed (hundreds of keV) electrons during substorms lead to whistler mode chorus wave generation and subsequent acceleration of the seed population to relativistic, and potentially ultra-relativistic (Allison et al., 2021), energies *via* local wave-particle interactions (e.g., Meredith et al., 2002), on a relatively rapid timescale. An illustration of this concept is provided in **Figure 6** (Jaynes et al., 2015). Meanwhile, radial diffusion progressively redistributes the newly created MeV population, smoothing out the PSD radial profile and providing additional energy to the MeV particles transported inward.

In summary, the picture of electron radiation belt acceleration has evolved over time in response to measurements from new missions in the Earth's inner magnetosphere, most notably thanks to the NASA Combined Release and Radiation Effects Satellite (CRRES) in the 1990s and most recently, the NASA THEMIS and the Van Allen Probes. In comparison, the magnetospheres of the outer planets are lacking data to differentiate between the leading processes for electron radiation belt acceleration, as summarized below.

3.2 Differentiating Between the Leading Processes for Electron Radiation Belt Acceleration at the Outer Planets

The magnetospheres of the four strongly magnetized outer planets (Jupiter, Saturn, Uranus, and Neptune) are hosts to electron radiation belts that display considerable differences from those of the Earth, namely energetic electron distributions that permanently extend to energies in excess of 70 MeV at Jupiter or 20 MeV at Saturn (Bolton et al., 2002; Kollmann et al., 2011). In addition, there is a large diversity of acceleration modes not resolved in the terrestrial geospace, largely due to those planets' strong magnetic fields, fast rotation, and large amounts of neutral material within their volume (Roussos and Kollmann, 2021). A consensus on the role of adiabatic against local electron acceleration at the outer planets is thus still pending, especially since the challenges in measuring comprehensively these systems are even higher than at Earth (Roussos et al., 2018b).

Specifically, almost all *in-situ* energetic electron observations at the outer planet radiation belts are single point measurements. This means that crossings of the radiation belts occur typically between several days to few weeks after the seed electron population in the middle and outer magnetosphere and/or the

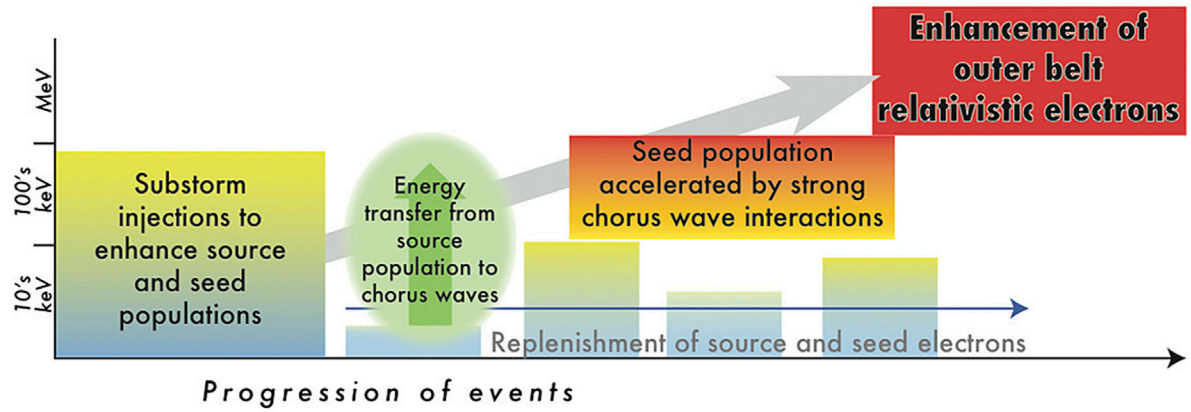

FIGURE 6 | Sequence for MeV acceleration by chorus waves in the Earth's outer radiation belt (from Jaynes et al., 2015).

solar wind has been sampled. Several methods that offer an indirect, quasi-regular monitoring of the seed regions (Tsuchiya et al., 2011; Murakami et al., 2016; Roussos et al., 2018a; Han et al., 2018; Bradley et al., 2020) reveal correlated appearances of MeV electron radiation belt transients at Jupiter and Saturn in response to episodic events in the outer magnetosphere, originating from internally-driven dynamics, or in the solar wind (Tsuchiya et al., 2011; Roussos et al., 2018b; Yuan et al., 2020). Such correlations alone, however, have proven insufficient to attribute the generation of transient populations to local or adiabatic acceleration. Another constraint derives from the difficulty to obtain energy-resolved measurements at all outer planets for electrons above ~1 MeV. As a consequence, available PSD electron profiles are largely limited to the sub-relativistic range (Kollmann et al., 2011; Ma et al., 2018), with only few exceptions where estimates of the macroscopic characteristics of electron spectra into the ultra-relativistic range (e.g., spectral slope) have been determined (e.g., Selesnick et al., 1997; Mihalov et al., 2000; Kollmann et al., 2018; Garrett and Jun 2021).

Despite the limitations, significant progress has been achieved in understanding electron acceleration at the outer planets, particularly at Jupiter and Saturn, thanks to extensive observations by the Galileo, Juno, and Cassini orbiters. Long-term imaging of the Jovian radiation belts in radio wavelengths also provides key evidence (de Pater and Goertz. 1990; Bolton et al., 2002). On average, adiabatic radial inward transport is important at the outer extension of both Jupiter's ($L > 10$) and Saturn's ($3.5 < L < 10$) electron belts (Kollmann et al., 2011, 2018; Roussos et al., 2018b; Ma et al., 2018; Sun et al., 2019, 2021; Paranicas et al., 2020; Yuan et al., 2021). This picture emerges either from mapping both the steady-state configuration of each electron belt, or by observing the temporal evolution of their perturbed states (e.g., Roussos et al., 2010). Radial transport can occur in various modes and be triggered by a variety of processes, such as ULF waves (Van Allen et al., 1980; Roussos et al., 2007), centrifugal interchange instability (Thorne et al., 1997; Mauk et al., 2005), transport by variable, large scale coherent plasma flows (Hao et al., 2020), or even solar wind transients.

The potential for local acceleration in the outer electron belt regions by whistler-mode chorus waves has been explored mostly through simulations (Shprits et al., 2012; Woodfield et al., 2014, 2019), but observationally, the case of important or even dominant contributions by local heating is even stronger for the innermost portion of the electron belts. The strong magnetic field and the low plasma densities in the inner jovian and saturnian magnetospheres generate an environment that is conducive to a continuous relativistic electron acceleration by Z-mode waves (Woodfield et al., 2018). Support for this case exists particularly for Saturn, in the form of butterfly pitch angle distributions (Yuan et al., 2021), and by simulations for Jupiter (Nénon et al., 2017). Even if local acceleration may be dominant at low L-shells, observations at both Jupiter and Saturn indicate that adiabatic transport is still a non-negligible regulator of the belts' state and dynamics. Episodes of strong electron enhancements in Jupiter's synchrotron belts have been attributed to periods of amplified radial diffusion rates (Miyoshi et al., 2000; Tsuchiya et al., 2011), triggered by periods of solar UV heating of the planet's thermosphere. These and many other observations (e.g., Louarn et al., 2014, 2016), indicate that the interplay between local and adiabatic heating at the outer planet electron belts likely changes with time and across a variety of temporal and spatial scales. Finally, local acceleration may also be important in generating the seed electron population of the radiation belts at Jupiter and Saturn. Impulsive injections of (ultra)relativistic electrons have been observed in the outer magnetospheres of both planets (Simpson et al., 1992; Mauk et al., 2005; Roussos et al., 2016; Palmaerts et al., 2016; Clark et al., 2017), but neither the acceleration process nor the fate of these electrons is yet fully resolved.

3.3 Solving the Radiation Belt dynamic Puzzle: A Multi-Faceted Challenge

While the role played by whistler-mode chorus waves in radiation belt acceleration is now well accepted at Earth, defining its relative importance remains controversial. In other words, we still do not know the percentage of radiation belt acceleration due to local acceleration *via* chorus wave-particle interactions. In the following, we highlight some of the major challenges to remove ambiguities and answer this question.

3.3.1 A Time-Varying Puzzle

First, the overall radiation belt dynamics result from concurrent processes that can influence each other and whose individual contributions are difficult to evaluate and time-varying (e.g., Tu et al., 2009; Xiang et al., 2021). Thus, any uncertainty in the magnitude of a source or loss process leads to other uncertainties in the magnitude of other processes.

In this context, it is also critical to quantify the losses that contribute to the "*Losses*" term in **Eq. 6** to fully understand acceleration events. Losses can be created internally *via* wave-particle pitch-angle scattering or ULF wave effects, resulting in atmospheric precipitation, or at the outer boundary of the magnetosphere, a process known as magnetopause shadowing (Turner et al., 2012), resulting in losses to the interplanetary medium. Radiation belt electrons are susceptible to pitch-angle scattering by three main wave modes: broadband VLF hiss, electromagnetic ion cyclotron (EMIC) waves, and coherent VLF chorus (Thorne et al., 2005). Hiss losses are most relevant within the dense plasmasphere region where hiss can persist (Thorne et al., 1979), although this loss mechanism becomes less important during active times when the plasmapause location can move inward on short timescales (Goldstein et al., 2005). When this happens, the particle distribution that was within the plasmasphere is suddenly outside and susceptible to other loss or acceleration processes. Electron lifetimes within the plasmasphere have been estimated using both theoretical and observational techniques (Jaynes et al., 2014; Orlova et al., 2014; Claudepierre et al., 2020). Hiss-driven loss is considered to be a slower, steady loss rather than an impulsive event. On the other hand, EMIC waves can cause intense, sudden scattering that manifests as localized depletions, and are thought to be a primary loss factor of relativistic and ultra-relativistic electrons in the heart of the outer radiation belts (Drozdov et al., 2021b). VLF chorus waves also scatter outer belt electrons efficiently, particularly in the ring current energy range (Shprits et al., 2007b). Microbursts, trains of which may be created by quasi-periodic chorus waves typically seen in the outer radiation belt, can cause relativistic losses in concert with lower energy loss due to wave propagation to higher latitudes (Miyoshi et al., 2020). Relativistic losses can also be contributed by the phenomenon referred to as dusk-side relativistic electron precipitation (Comess et al., 2013), which are driven by both microburst events and non-microburst events. Microburst trains may be long-lasting, as evidenced by their connection to pulsating aurora which can be long-duration and widespread (Jones et al., 2013), and therefore may be a significant loss process for relativistic outer belt electrons. Finally, ULF waves have been implicated in energetic electron losses through a mechanism by which the radial oscillatory motion causes a lowering of the mirror point in a modulated manner (Brito et al., 2012). Taken together, these effects contribute to a net loss term in the characterization of the outer radiation belt system, and must be accounted for in order to accurately quantify the acceleration terms.

In addition, an accurate determination of the location of the last closed drift shell is an important parameter to include in Earth's radiation belt modeling as it contributes to radiation belt losses during active times. Yet it requires assuming an instantaneous magnetic field topology, including the magnetopause location (e.g., Albert et al., 2018; Olifer et al., 2018; Staples et al., 2020), and the accuracy of such assumption is hard to quantify. In addition, diffusion coefficients require knowledge of instantaneous field variations and plasma conditions all along the trapped particles' drift shell, including plasmapause location (e.g., Malaspina et al., 2016, 2020; Wang et al., 2020). For the energy diffusion coefficient, this means knowing the chorus wave spectral intensity, amplitude, and plasma density at all magnetic local times over the drift shell in real time (Thorne et al., 2013; Allison et al., 2021). For the radial diffusion coefficient, this means knowing instantaneous electric and magnetic field variations all along the drift contour (e.g., Lejosne and Kollmann, 2020). Thus, assumptions need to be made, and averaged conditions are usually preferred. As a result, diffusion coefficients are often parameterized in terms of magnetic activity indices, smoothing out estimated errors as well as natural variability (e.g., Watt et al., 2017). Yet, the need for "event-specific" diffusion coefficients is now well recognized (e.g., Tu et al., 2009) and efforts have been made to provide such information (Tu et al., 2012; Li Z. et al., 2017; Lejosne, 2020; Ozeke et al., 2020).

That said, converting measurements into inputs to the 3D Fokker-Planck equation means complying with the presupposed diffusion framework (**Section 2.3**), an increasingly complicated task as data resolution improves.

3.3.2 Challenging the Applicability of Our Current Radiation Belt Master Equation: A Local Peak in the PSD Radial Profile is not Conclusive Evidence for Local Acceleration

Most counter-arguments to local acceleration as the prevailing radiation belt acceleration mechanism challenge the interpretation of experimental data resulting in a peak in the PSD radial profile. These counter-arguments boil down to two main reasons.

The first is technical: Mapping measurements into phase space requires assuming a magnetic field model, whose real-time accuracy is difficult to quantify (see also the review by Green (2006) for methods to obtain PSD estimates). Let us also mention that the DC and low frequency electric fields can affect the dynamics of source and seed particles (tens to hundreds of keV): They can distort trapped particle drift shells, thereby modifying their third adiabatic coordinate L^*.

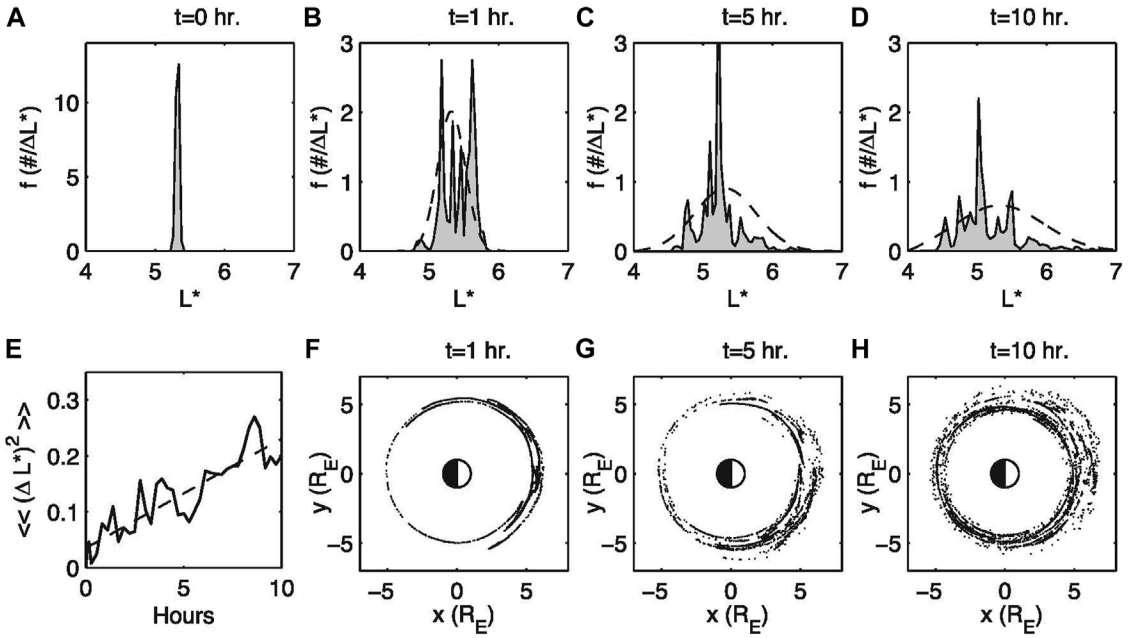

FIGURE 7 | Time evolution of a normalized distribution function, *f*, during a test particle simulation including 10,000 equatorial guiding centers injected in electric and magnetic fields provided by the Lyon-Fedder-Mobarry (LFM) global MHD simulation code (Lyon et al., 2004) during a 10 h time interval (3 January 2003) with "nothing unusual" (solar wind speed ~ 550 *km/s*, density ~ 10 cm^{-3} and IMF B_z fluctuating between ± 10 nT). The distribution is **(A)** initially radially localized at $L^* = 5.3$, and it spreads over time in L* **(B–D)**, to encapsulate the time evolution of the locations of the tracked test particles **(F–H)**. The time evolution of the distribution function representing the test particles is compared to the time evolution of the solution of the diffusion equation [dash lines in panels **(B–D)**], highlighting significant discrepancies, even after many drift periods (from Kress et al., 2012).

While this effect has been observed and studied for tens to hundreds of keV electrons in the Earth's inner belt (e.g., Selesnick et al., 2016; Lejosne et al., 2021), drift shell distortion by large-scale electric fields is reasonably omitted when it comes to defining the adiabatic coordinates of MeV particles in the Earth's outer radiation belt. Even when so, the conversion of experimental data into phase space density (PSD) parameterized by adiabatic coordinates remains a pitfall (e.g., Selesnick and Blake, 2000; Green and Kivelson, 2004). In particular, errors in magnetic field models can lead to the apparition of an artificial peak in the PSD radial profile, which vanishes when a realistic magnetic field model is used (e.g., Loridan et al., 2019). In addition, transient PSD peaks can also be spatio-temporal artifacts that disappear when leveraging multipoint measurements (e.g., Olifer et al., 2021). One way to test magnetic field model accuracy is to compare magnetic field model outputs and *in-situ* magnetic field measurements when available (e.g., Ozeke et al., 2019). In addition, the detection of a growing local peak requires observations during the acceleration process. Yet, the time resolution of *in-situ* measurements is constrained by spacecraft orbit period or revisit time.

The second reason is physical: Radial transport dynamics can also generate a local peak in the PSD radial profile (e.g., Ukhorskiy et al., 2006; Degeling et al., 2008), thereby further questioning the appropriateness of summarizing radial transport in terms of a diffusion process in the radiation belt master equation (**Eq. 7**) (e.g., Elkington et al., 1999; Kress et al., 2012, **Figure 7**).

In fact, a comparison between diffusion and particle drift descriptions of radial transport showed that the two modeling choices provide best agreement in the case of a series of sequential small storms and mediocre agreement during event analysis (Riley and Wolf, 1992). This is also why case events associated with fast radial transport (injection or drift resonance) are usually modeled by tracking test particles (i.e., guiding centers) drifting in analytical descriptions of the wave-associated electric field (e.g., Zong et al., 2017; Zong, 2022) or in MHD fields (e.g., Hudson et al., 2017). In contrast, summarizing local wave particle interactions in terms of diffusion in energy and pitch angle appears more reasonable (e.g., Tao et al., 2012), even though nonlinear effects occur in the presence of intense chorus waves, routinely measured *in-situ* (e.g., Zhang et al., 2019). In that context, alternative methods have been proposed to summarize the effect of chorus wave particle interactions on distribution functions (e.g., Furuya et al., 2008; Kubota and Omura, 2018; Artemyev et al., 2020).

While adjustments to the Fokker-Planck framework have been proposed to improve the description of trapped particle radial transport on timescales smaller than the drift period for the radiation belts (e.g., Bourdarie et al., 1997; Shprits et al., 2015) and for the ring current population (e.g., Fok et al., 2014; Jordanova

***Table A:* A Summary of the Approach**

Objective: Interpreting Measurements to Differentiate between Leading Acceleration Mechanisms	
Requirements	• ***Observations***: Energy and pitch angle resolved measurements over a time interval during which acceleration occurs • ***Discriminability for the acceleration processes***: Different acceleration mechanisms must have different signatures in measurements in order to be able to differentiate them
Applications	• ***Observations*:** Flux, transformed into phase space density (PSD) • ***Interpretation, based on a 3D diffusion driven model*** (**Table C**): A growing peak in the radial profile of the PSD is interpreted as a signature of local acceleration, while radial diffusion is expected to smooth out radial gradients
Drawbacks	• ***Observations***: Data resolution + data processing (***Table B2***) constrain the approach • ***Interpretation*:** Based on a limited representation of radiation belt dynamics (***Table C***). Uncertainty as to where and when the leading acceleration processes results in different, identifiable signatures. This ambiguity results in controversies

***Tables B:* (B1) Observations Should be Converted into (B2) Adiabatic Space**

(B1) Observation: Electron Flux Enhancement	
Interpretation	• Radiation belt acceleration
Assumption	• More particles at lower energies. Thus, a greater flux indicates accelerated particles
Drawback	• Special circumstances under which the assumption is not valid (e.g. Bump-On-Tail distribution)

(B2) Data Product: Phase Space Density Mapped in Adiabatic Coordinates	
Requirements	• Choosing magnetic & electric field models • Specifying the adiabatic coordinates
Advantage	• Disentangling adiabatic from non-adiabatic effects
Drawbacks	• Inaccuracy associated with mapping into adiabatic space (model uncertainty) • Populations on open drift shells, open field lines, etc. excluded from the study (undefined adiabatic coordinates)

***Table C:* A Modeling Framework is Needed to Interpret Observations**

Model: 3D Fokker-Planck Equation in Adiabatic Space	
Requirements	• Specifying inputs (providing boundary conditions, including lower energy boundary, source, loss, diffusion coefficients) • Assuming diffusion (i.e., assuming that the overall effects of most processes modifying the population adiabatic coordinates can be encapsulated by diffusion coefficients)
Advantages	• Practical (modeling enabled and simplified) • Operational (dynamics over long time intervals can be reproduced, from months to years)
Drawbacks	• Uncertainty associated with input quantification • Cannot render non-diffusive effects (e.g., injections, non linear effects) • Coarse spatio-temporal resolution: Cannot model radiation belt dynamics on a timescale shorter than that of drift phase mixing. Cannot reproduce magnetic local time variations • No systematic knowledge of where and when the modeling assumptions are valid

FIGURE 8 | A summary chart on the challenges associated with differentiating between the leading processes for electron radiation belt acceleration.

et al., 2016), they also call for improved experimental knowledge of the electric and magnetic field variations driving radiation belt dynamics.

In summary, the appropriateness of our current master equation for modeling radiation belt dynamics has limitations, in particular when it comes to rendering the effects of radial transport on radiation belt dynamics on short time scales. In the absence of a modeling framework able to account for the effects of both diffusive and non-diffusive (i.e., coherent) radial transport, as well as for the effects of local acceleration (including non-linear regimes), it is not possible to quantify unequivocally the importance of local acceleration versus large-scale acceleration associated with radial transport. While the Fokker-Planck formalism has done well for long-term radiation belt modeling, it appears to be insufficient for definitive event analysis during active times. Thus, care must be taken when drawing conclusions on the physics at play solely based on PSD dynamics, and even more so on flux dynamics.

4 DISCUSSION

A summary of the challenges to address when interpreting measurements to differentiate between electron radiation belt leading acceleration mechanisms is provided in **Figure 8**. It is detailed and discussed below (**Section 4.1**). Suggestions for future research directions are provided in **Section 4.2**.

4.1 Topic Overview

The first challenge in discussing radiation belt electron acceleration is data procurement: Time series of flux measurements are needed to analyze radiation belt dynamics. It is indeed thanks to improved data sets from new missions that the picture of electron radiation belt acceleration in the Earth's magnetosphere has evolved over time. In contrast, the magnetospheres of the outer planets are still lacking key data to fully differentiate between the leading processes for electron radiation belt acceleration (**Section 3.2**). The measured electron flux time variations inform on the governing processes controlling radiation belt dynamics. That said, the experimental information is sparse as it mainly consists of samples along spacecraft trajectory. In addition, electron flux time variations only represent the *net result* of a variety of source and loss processes acting, and possibly interacting, concurrently. In that context, it is necessary to rely on a theoretical framework to determine how to identify and quantify the effect of each source and loss process.

Electron flux enhancements are readily associated with times during which acceleration processes dwarf losses. The equivalence between flux enhancement and trapped particle acceleration relies on the assumption that the accelerated particles correspond to a greater flux, i.e., that there are more particles at lower energies. While special cases such as bump-on-tail distributions challenge this assumption, they are unexpected. Bump-on-tail distributions for instance are usually observed in the plasmasphere at $L > 2.5$ during relatively quiet times (e.g., Zhao et al., 2019c) and are attributed to interactions with plasmaspheric hiss waves.

Times when radiation belt particles are accelerated are times during which the fields provide energy to the particles. Since the magnetic force does no work, it is the electric field that conveys energy. Because the electric field component parallel to the magnetic field direction is generally null, the focus is mainly on energization by perpendicular electric fields. That said, observations of large oblique chorus waves and time domain structures (TDS) in the outer belt indicate that transient parallel electric fields can also efficiently energize electrons, rapidly producing seed populations (e.g., Agapitov et al., 2015; Mozer et al., 2015, 2016). On the other hand, radiation belt acceleration produced by perpendicular electric fields occurs along the circle of gyration (gyro-betatron), and along the drift contour (drift betatron). It can be such that the adiabatic coordinates are conserved (e.g., **Figure 2**, see also Fillius and McIlwain, 1967) or violated.

Many candidate radiation belt acceleration mechanisms have been proposed over the years to account for the violation of one or several of the adiabatic coordinates parameterizing a trapped radiation belt electron population (see for instance the review by (Friedel et al., 2002), for details). Yet, the focus remains on 1) local acceleration by VLF whistler-mode chorus waves at the gyro-scale, and 2) global acceleration associated with radial transport by ULF waves at the drift-scale. Because these two mechanisms occur on two very different scales, their efficiency is usually quantified independently. On one hand, dividing radiation belt acceleration research between studies of local vs. global mechanisms is a convenient and efficient way to approach the problem, and adiabatic invariant theory provides an appropriate framework to do so. On the other hand, the divide is artificial, and it runs the risk of generating silos. Chorus and ULF waves can be concurrent (e.g., O'Brien et al., 2003) and possibly act in synergy (e.g., Simms et al., 2018, 2021). In addition, local processes can have global consequences as trapped particles continuously gyrate, bounce, and drift around the planet. For instance, pitch angle scattering of a trapped population in presence of drift shell splitting generates radial transport (e.g., Schulz, 1972). Yet, such effects—together with other "off-diagonal terms" of the diffusion tensor – are commonly omitted in radiation belt models, in part because of the numerical challenges that they pose (e.g., O'Brien, 2014; Zheng et al., 2016). It is also worth pointing out that interactions with VLF and ULF waves energize some part of the trapped population while de-energizing and/or contributing to the loss of another part of the population (e.g., Li W. et al., 2007; Shprits et al., 2006, 2008; Drozdov et al., 2020). Thereby, they act simultaneously as source and loss mechanisms for the trapped population. In this context, the efficiency of trapped particle interactions with VLF and ULF waves is usually encapsulated in the form of a few diffusion coefficients (and sometimes a lifetime coefficient), assuming a quasi-linear regime. These coefficients are then used as inputs for a physics-based radiation belt model that is diffusion-driven, and which consists of solving a 3D Fokker-Planck equation in adiabatic space.

Describing radiation belt dynamics by solving the 3D Fokker-Planck equation in adiabatic space remains the favored radiation

belt modeling approach because it is the most computationally efficient. It offers a relatively accessible way to render radiation belt dynamics while meeting the space weather needs for long term radiation belt modeling. In addition, it has proven to do well during geomagnetic quiet times. That said, it requires electron flux measurements to be converted into phase space density (PSD) mapped in adiabatic invariant space, to provide boundary conditions and to perform model-observation comparisons. This mapping inevitably adds uncertainty and limitation to the analysis (**Section 3.3.2**). In addition, the quasi-linear diffusive model does not necessarily provide a realistic picture of the physics of wave-particle interactions: Non-diffusive effects are left out from the analysis, by design (**Section 2.3.2**). This means for instance that the model is ill-suited to render times when particle dynamics are coherent (e.g., significant particle injections). The location of the outer boundary is also limited to the location of the last closed drift shell. Yet, modeling particle trapping beyond the outer boundary (i.e., dealing with populations with undefined adiabatic coordinates in the trapping region) is a requirement when the objective is to connect radiation belt populations to their outer source (e.g., energetic electrons in the magnetotail—Turner et al., 2021).

It is by relying on the interpretative framework provided by the solution of the 3D Fokker-Planck equation that measurements are analyzed to differentiate between leading acceleration mechanisms (**Figure 8A**). Observations of a growing peak in the radial profile of the PSD data product during enhancement events have been repeatedly interpreted as a telltale signature of local acceleration because radial diffusion can only smooth the PSD radial profile (e.g., Allison and Shprits, 2020). While a consensus appears to have emerged, ambiguities remain because of the set of limits associated with both data processing (**Figure 8B**) and theoretical framework (**Figure 8C**).

In particular, radial transport does not appear to be well described by a diffusive approximation during active times (**Section 3.3.2**). Drift echoes are experimental signatures of radial transport that can be observed when particles detectors have sufficiently high energy resolution (e.g., Hartinger et al., 2018; Hudson et al., 2020; Zhao et al., 2021). Yet they cannot be rendered by diffusion-driven radiation belt models. In the absence of a modeling framework able to account for 1) the effects of both diffusive and non-diffusive (i.e., rapid, significant and coherent) radial transport, as well as 2) the effects of local acceleration (including nonlinear effects), it is not possible to quantify the importance of local vs. radial acceleration unequivocally. Given current computational advances, time may have come to go beyond a purely diffusion-driven model, towards a more realistic modeling framework (e.g., Artemyev et al., 2021; Lukin et al., 2021; Allanson et al., 2022). That said, improved radiation belt modeling would also require improved knowledge of the characteristics of trapped particle interactions with VLF and ULF waves—*via* experimental determination of the correlation decay time for instance (e.g., Ukhorskiy and Sitnov, 2013). Currently, much work still remains to be done even when it comes to reducing uncertainty in the inputs for the 3D Fokker-Planck equation, including diffusion coefficients (e.g., Drozdov et al., 2021a). Thus, much remains to be done to quantify the importance of local vs. radial acceleration unambiguously.

4.2 Suggested Future Research Directions

Recent work discussed in **Section 3.3** suggests that many of the unresolved questions relating to the relative importance of radial transport and local acceleration could be addressed through expanded networks of multi-point observations. For example, Olifer et al. (2021) showed that when two Van Allen Probes spacecraft sample the same region of phase space in rapid succession, ambiguities concerning the origin of a local peak in radial PSD profile can be removed. Expanded constellations of satellites with similar orbits to the Van Allen Probes would further reduce ambiguities concerning the persistence of local PSD peaks and their origin; with each additional spacecraft added, processes that occur on shorter timescales and smaller spatial scales can be examined (e.g., Staples et al., 2022). Expanded networks of satellites with magnetic field, electric field, and energetic particle measurements would also provide 1) more robust constraints for magnetic field models used to obtain PSD, 2) more robust constraints for radiation belt models that require particle measurements for their boundary conditions, and 3) better information concerning global wave properties that are frequently used to both constrain radiation belt models and also provide diagnostics of the acceleration process. 1), 2), and 3) are all crucial for understanding dynamics during events with rapidly evolving features in radial PSD profiles. Even in the case of the Earth's radiation belts, there are still a few regions that are particularly undersampled, including Low Earth Orbit up to >1000 km ("High LEO"), and High-Inclination orbits where particle measurements could be used to distinguish between the dynamics of trapped, quasi-trapped, and precipitating particles. Finally, expanded networks of ground-based measurements could be used to remote sense global wave fields (e.g., magnetometers) and provide information about precipitating particles with different energies (e.g., riometers, incoherent scatter radars, all sky cameras), providing important constraints that supplement sparse satellite measurements, for example, networks of ground magnetometers have already proved essential in accurately capturing event-specific ULF wave power. To summarize, we already know from recent work that additional satellites and ground-based measurements can yield new insight into the relative importance of local acceleration and radial transport; we thus expect that future studies using expanding networks of multi-point observations would be able to probe dynamics on shorter timescales than were possible before (reduced satellite revisit time in radial PSD profile), more accurately than was possible before (better constraints on PSD and related magnetic field models), and with less uncertainty concerning the underlying processes causing acceleration (global, event-specific wave constraints).

AUTHOR CONTRIBUTIONS

The first author is the lead and corresponding author. All other authors are listed in alphabetical order. We describe

contributions to the paper using the CRediT (Contributor Roles Taxonomy) categories (Brand et al., 2015). Conceptualization: All authors. Writing—Original Draft: SL, HJA, MDH, ANJ, and ER. Writing—Review and Editing: All authors.

FUNDING

SL work was performed under NASA Grant 80NSSC18K1223. HA acknowledges support from the Alexander von Humboldt Foundation. LWB work was performed under NASA Grant 80NSSC21K1314. AYD contribution acknowledges NASA grant 80NSSC18K0663. MDH work was performed under NASA Grant 80NSSC19K0907. MKH contribution acknowledges NASA Grant 80NSSC17K0678. HZ was supported by the NSF Grant AGS 2140933 and NASA Grant 80NSSC22K0473.

ACKNOWLEDGMENTS

SL thanks Professor Jacob Bortnik for helping with **Figure 4**.

REFERENCES

Agapitov, O. V., Artemyev, A. V., Mourenas, D., Mozer, F. S., and Krasnoselskikh, V. (2015). Nonlinear Local Parallel Acceleration of Electrons through Landau Trapping by Oblique Whistler Mode Waves in the Outer Radiation Belt. *Geophys. Res. Lett.* 42 (10140–10), 149. doi:10.1002/2015GL066887

Albert, J. M. (2002). Nonlinear Interaction of Outer Zone Electrons with VLF Waves. *Geophys. Res. Lett.* 29 (8), 116–121. doi:10.1029/2001GL013941

Albert, J. M., Selesnick, R. S., Morley, S. K., Henderson, M. G., and Kellerman, A. C. (2018). Calculation of Last Closed Drift Shells for the 2013 GEM Radiation Belt Challenge Events. *J. Geophys. Res. Space Phys.* 123, 9597–9611. doi:10.1029/2018JA025991

Ali, A. F., Malaspina, D. M., Elkington, S. R., Jaynes, A. N., Chan, A. A., Wygant, J., et al. (2016). Electric and Magnetic Radial Diffusion Coefficients Using the Van Allen Probes Data. *J. Geophys. Res. Space Phys.* 121, 9586–9607. doi:10.1002/2016JA023002

Allanson, O., Elsden, T., Watt, C., and Neukirch, T. (2022). Weak Turbulence and Quasilinear Diffusion for Relativistic Wave-Particle Interactions via a Markov Approach. *Front. Astronomy Space Sci.* 8. doi:10.3389/fspas.2021.805699

Allanson, O., Watt, C. E. J., Ratcliffe, H., Meredith, N. P., Allison, H. J., Bentley, S. N., et al. (2019). Particle-in-cell Experiments Examine Electron Diffusion by Whistler-mode Waves: 1. Benchmarking with a Cold Plasma. *J. Geophys. Res. Space Phys.* 124, 8893–8912. doi:10.1029/2019ja027088

Allison, H. J., and Shprits, Y. Y. (2020). Local Heating of Radiation Belt Electrons to Ultra-relativistic Energies. *Nat. Commun.* 11, 4533. doi:10.1038/s41467-020-18053-z

Allison, H. J., Shprits, Y. Y., Zhelavskaya, I. S., Wang, D., and Smirnov, A. G. (2021). Gyroresonant Wave-Particle Interactions with Chorus Waves during Extreme Depletions of Plasma Density in the Van Allen Radiation Belts. *Sci. Adv.* 7 (5), eabc0380. doi:10.1126/sciadv.abc0380

Artemyev, A. V., Neishtadt, A. I., and Vasiliev, A. A. (2020). Mapping for Nonlinear Electron Interaction with Whistler-Mode Waves. *Phys. Plasmas* 27, 042902. doi:10.1063/1.5144477

Artemyev, A. V., Neishtadt, A. I., Vasiliev, A. A., Zhang, X.-J., Mourenas, D., and Vainchtein, D. (2021). Long-term Dynamics Driven by Resonant Wave-Particle Interactions: from Hamiltonian Resonance Theory to Phase Space Mapping. *J. Plasma Phys.* 87, 835870201. doi:10.1017/S0022377821000246

Baker, D. N., Belian, R. D., Higbie, P. R., Klebesadel, R. W., and Blake, J. B. (1987). Deep Dielectric Charging Effects Due to High-Energy Electrons in Earth's Outer Magnetosphere. *J. Electrost.* 20 (1). doi:10.1016/0304-3886(87)90082-9

Baker, D. N., Blake, J. B., Callis, L. B., Cummings, J. R., Hovestadt, D., Kanekal, S., et al. (1994). Relativistic Electron Acceleration and Decay Time Scales in the Inner and Outer Radiation Belts: SAMPEX. *Geophys. Res. Lett.* 21 (6), 409–412. doi:10.1029/93GL03532

Baker, D. N., Erickson, P. J., Fennell, J. F., Foster, J. C., Jaynes, A. N., and Verronen, P. T. (2018). Space Weather Effects in the Earth's Radiation Belts. *Space Sci. Rev.* 214. doi:10.1007/s11214-017-0452-7

Baker, D. N., Hoxie, V., Zhao, H., Jaynes, A. N., Kanekal, S., Li, X., et al. (2019). Multiyear Measurements of Radiation Belt Electrons: Acceleration, Transport, and Loss. *J. Geophys. Res. Space Phys.* 124, 2588–2602. doi:10.1029/2018JA026259

Baker, D. N., Kanekal, S. G., and Blake, J. B. (2004). Characterizing the Earth's Outer Van Allen Zone Using a Radiation Belt Content Index. *Space weather.* 2 (2). doi:10.1029/2003sw000026

Baker, D. N., Kanekal, S. G., Hoxie, V., Li, X., Jaynes, A. N., Zhao, H., et al. (2021). The Relativistic Electron-Proton Telescope (REPT) Investigation: Design, Operational Properties, and Science Highlights. *Space Sci. Rev.* 217, 68. doi:10.1007/s11214-021-00838-3

Baker, D. N., Li, X., Turner, N., Allen, J. H., Bargatze, L. F., Blake, J. B., Sheldon, R. B., Spence, H. E., Belian, R. D., Reeves, G. D., Kanekal, S. G., Klecker, B., Lepping, R. P., Ogilvie, K., Mewaldt, R. A., Onsager, T., Singer, H. J., and Rostoker, G. (1997). Recurrent Geomagnetic Storms and Relativistic Electron Enhancements in the Outer Magnetosphere: ISTP Coordinated Measurements. *J. Geophys. Res.* 102 (A7), 14141–14148. doi:10.1029/97ja00565

Beutier, T., and Boscher, D. (1995). A Three-Dimensional Analysis of the Electron Radiation Belt by the Salammbô Code. *J. Geophys. Res.* 100 (A8), 14853–14861. doi:10.1029/94JA03066

Blake, J. B., Baker, D. N., Turner, N., Ogilvie, K. W., and Lepping, R. P. (1997). Correlation of Changes in the Outer-Zone Relativistic-Electron Population with Upstream Solar Wind and Magnetic Field Measurements. *Geophys. Res. Lett.* 24 (NO.8), 927–929. doi:10.1029/97GL00859

Bolton, S. J., Janssen, M., Thorne, R., Levin, S., Klein, M., Gulkis, S., et al. (2002). Ultra-relativistic Electrons in Jupiter's Radiation Belts. *Nature* 415, 987–991. doi:10.1038/415987a

Bortnik, J., Thorne, R. M., and Inan, U. S. (2008). Nonlinear Interaction of Energetic Electrons with Large Amplitude Chorus. *Geophys. Res. Lett.* 35, L21102. doi:10.1029/2008GL035500

Bortnik, J., Thorne, R. M., Li, W., and Tao, X. (2016). "Chorus Waves in Geospace and Their Influence on Radiation Belt Dynamics," in *Waves, Particles, and Storms in Geospace: A Complex Interplay*, 192–216. doi:10.1093/acprof:oso/9780198705246.003.0009

Bourdarie, S., Boscher, D., Beutier, T., Sauvaud, J.-A., and Blanc, M. (1997). Electron and Proton Radiation Belt Dynamic Simulations during Storm Periods: A New Asymmetric Convection-Diffusion Model. *J. Geophys. Res.* 102 (A8), 17541–17552. doi:10.1029/97JA01305

Boyd, A. J., Turner, D. L., Reeves, G. D., Spence, H. E., Baker, D. N., and Blake, J. B. (2018). What Causes Radiation Belt Enhancements: A Survey of the Van Allen Probes Era. *Geophys. Res. Lett.* 45, 5253–5259. doi:10.1029/2018GL077699

Bradley, T. J., Cowley, S. W. H., Bunce, E. J., Melin, H., Provan, G., Nichols, J. D., et al. (2020). Saturn's Nightside Dynamics during Cassini's F Ring and Proximal Orbits: Response to Solar Wind and Planetary Period Oscillation Modulations. *J. Geophys. Res. Space Phys.* 125, e27907. doi:10.1029/2020JA027907

Brand, A., Allen, L., Altman, M., Hlava, M., and Scott, J. (2015). Beyond Authorship: Attribution, Contribution, Collaboration, and Credit. *Learn. Pub.* 28, 151–155. doi:10.1087/20150211

Brautigam, D. H., and Albert, J. M. (2000). Radial Diffusion Analysis of Outer Radiation Belt Electrons during the October 9, 1990, Magnetic Storm. *J. Geophys. Res.* 105 (A1), 291–309. doi:10.1029/1999JA900344

Brito, T., Woodger, L., Hudson, M., and Millan, R. (2012). Energetic Radiation Belt Electron Precipitation Showing ULF Modulation. *Geophys. Res. Lett.* 39 (22). doi:10.1029/2012gl053790

Bruff, M., Jaynes, A. N., Zhao, H., Goldstein, J., Malaspina, D. M., Baker, D. N., et al. (2020). The Role of the Dynamic Plasmapause in Outer Radiation Belt Electron

Flux Enhancementflux Enhancement. *Geophys. Res. Lett.* 47, e2020GL086991. doi:10.1029/2020GL086991

Camporeale, E. (2015). Resonant and Nonresonant Whistlers-Particle Interaction in the Radiation Belts. *Geophys. Res. Lett.* 42, 3114–3121. doi:10.1002/2015GL063874

Chen, Y., Reeves, G. D., and Friedel, R. H. W. (2007). The Energization of Relativistic Electrons in the Outer Van Allen Radiation Belt. *Nat. Phys.* 3, 614–617. doi:10.1038/nphys655

Chu, F., Hudson, M. K., Haines, P., and Shprits, Y. (2010). Dynamic Modeling of Radiation Belt Electrons by Radial Diffusion Simulation for a 2 Month Interval Following the 24 March 1991 Storm Injection. *J. Geophys. Res.* 115, a–n. doi:10.1029/2009JA014409

Claudepierre, S. G., Ma, Q., Bortnik, J., O'Brien, T. P., Fennell, J. F., and Blake, J. B. (2020). Empirically Estimated Electron Lifetimes in the Earth's Radiation Belts: Comparison with Theory. *Geophys Res. Lett.* 47 (3), e2019GL086056. doi:10.1029/2019GL086056

Comess, M. D., Smith, D. M., Selesnick, R. S., Millan, R. M., and Sample, J. G. (2013). Duskside Relativistic Electron Precipitation as Measured by SAMPEX: A Statistical Survey. *J. Geophys. Res. Space Phys.* 118 (8), 5050–5058. doi:10.1002/jgra.50481

de Pater, I., and Goertz, C. K. (1990). Radial Diffusion Models of Energetic Electrons and Jupiter's Synchrotron Radiation: 1. Steady State Solution. *J. Geophys. Res.* 95, 39. doi:10.1029/JA095iA01p00039

Degeling, A. W., Ozeke, L. G., Rankin, R., Mann, I. R., and Kabin, K. (2008). Drift Resonant Generation of Peaked Relativistic Electron Distributions by Pc 5 ULF Waves. *J. Geophys. Res.* 113, a–n. doi:10.1029/2007JA012411

Dessler, A. J., and Karplus, R. (1961). Some Effects of Diamagnetic Ring Currents on Van Allen Radiation. *J. Geophys. Res.* 66 (8), 2289–2295. doi:10.1029/JZ066i008p02289

Drozdov, A. Y., Allison, H. J., Shprits, Y. Y., Elkington, S. R., and Aseev, N. A. (2021a). A Comparison of Radial Diffusion Coefficients in 1-D and 3-D Long-Term Radiation Belt Simulations. *JGR Space Phys.* 126, e2020JA028707. doi:10.1029/2020JA028707

Drozdov, A. Y., Allison, H. J., Shprits, Y. Y., Usanova, M. E., Saikin, A. A., and Wang, D. (2021b). Depletions of Multi-MeV Electrons and Their Association to Minima in Phase Space Density. *Earth Space Sci. Open Archive* 19. doi:10.1002/essoar.10510085.1

Drozdov, A. Y., Blum, L. W., Hartinger, M., Zhao, H., Lejosne, S., Hudson, M. K., et al. (2022). Radial Transport versus Local Acceleration: The Long-Standing Debate. *Earth Space Sci.* 9, e2022EA002216. doi:10.1029/2022EA002216

Drozdov, A. Y., Shprits, Y. Y., Aseev, N. A., Kellerman, A. C., and Reeves, G. D. (2017). Dependence of Radiation Belt Simulations to Assumed Radial Diffusion Rates Tested for Two Empirical Models of Radial Transport. *Space weather.* 15, 150–162. doi:10.1002/2016SW001426

Drozdov, A. Y., Shprits, Y. Y., Orlova, K. G., Kellerman, A. C., Subbotin, D. A., Baker, D. N., et al. (2015). Energetic, Relativistic, and Ultrarelativistic Electrons: Comparison of Long-Term VERB Code Simulations with Van Allen Probes Measurements. *J. Geophys. Res. Space Phys.* 120, 3574–3587. doi:10.1002/2014JA020637

Drozdov, A. Y., Usanova, M. E., Hudson, M. K., Allison, H. J., and Shprits, Y. Y. (2020). The Role of Hiss, Chorus, and EMIC Waves in the Modeling of the Dynamics of the Multi-MeV Radiation Belt Electrons. *J. Geophys. Res. Space Phys.* 125 (9), 2628. doi:10.1029/2020JA028282

Elkington, S. R., Hudson, M. K., and Chan, A. A. (1999). Acceleration of Relativistic Electrons via Drift-Resonant Interaction with Toroidal-Mode Pc-5 ULF Oscillations. *Geophys. Res. Lett.* 26 (21), 3273–3276. doi:10.1029/1999GL003659

Fälthammar, C.-G. (1965). Effects of Time-dependent Electric Fields on Geomagnetically Trapped Radiation. *J. Geophys. Res.* 70 (11), 2503–2516. doi:10.1029/JZ070i011p02503

Fillius, R. W., and McIlwain, C. E. (1967). Adiabatic Betatron Acceleration by a Geomagnetic Storm. *J. Geophys. Res.* 72 (15), 4011–4015. doi:10.1029/JZ072i015p04011

Fok, M.-C., Buzulukova, N. Y., Chen, S.-H., Glocer, A., Nagai, T., Valek, P., et al. (2014). The Comprehensive Inner Magnetosphere-Ionosphere Model. *J. Geophys. Res. Space Phys.* 119, 7522–7540. doi:10.1002/2014JA020239

Fok, M. C. (2020). "Current Status of Inner Magnetosphere and Radiation Belt Modeling," in *Dayside Magnetosphere Interactions*. Editors Q. Zong, P. Escoubet, D. Sibeck, G. Le, and H. Zhang, 231–242. doi:10.1002/9781119509592.ch13

Foster, J. C., Erickson, P. J., Baker, D. N., Claudepierre, S. G., Kletzing, C. A., Kurth, W., et al. (2014). Prompt Energization of Relativistic and Highly Relativistic Electrons during a Substorm Interval: Van Allen Probes Observations. *Geophys. Res. Lett.* 41, 20–25. doi:10.1002/2013GL058438

Fox, N., and Burch, J. L. (2014). "The Van Allen Probes Mission," in *Physics and Astronomy* (Boston, MA: Springer). doi:10.1007/978-1-4899-7433-4

Friedel, R. H. W., Reeves, G. D., and Obara, T. (2002). Relativistic Electron Dynamics in the Inner Magnetosphere - a Review. *J. Atmos. Solar-Terrestrial Phys.* 64 (2), 265–282. doi:10.1016/S1364-6826(01)00088-8

Furuya, N., Omura, Y., and Summers, D. (2008). Relativistic Turning Acceleration of Radiation Belt Electrons by Whistler Mode Chorus. *J. Geophys. Res.* 113, a–n. doi:10.1029/2007JA012478

Garrett, H. B., and Jun, I. (2021). First Adiabatic Invariants and Phase Space Densities for the Jovian Electron and Proton Radiation Belts-Galileo and GIRE3 Estimates. *J. Geophys. Res. Space Phys.* 126, e28593. doi:10.1029/2020JA028593

Gendrin, R. (1981). General Relationships between Wave Amplification and Particle Diffusion in a Magnetoplasma. *Rev. Geophys.* 19, 171. doi:10.1029/rg019i001p00171

Ginet, G. P., O'Brien, T. P., Huston, S. L., Johnston, W. R., Guild, T. B., Friedel, R., et al. (2013). AE9, AP9 and SPM: New Models for Specifying the Trapped Energetic Particle and Space Plasma Environment. *Space Sci. Rev.* 179, 579–615. doi:10.1007/s11214-013-9964-y

Glauert, S. A., Horne, R. B., and Meredith, N. P. (2018). A 30-year Simulation of the Outer Electron Radiation Belt. *Space weather.* 16, 1498–1522. doi:10.1029/2018SW001981

Goldstein, J., Kanekal, S. G., Baker, D. N., and Sandel, B. R. (2005). Dynamic Relationship between the Outer Radiation Belt and the Plasmapause during March–May 2001. *Geophys. Res. Lett.* 32 (15). doi:10.1029/2005gl023431

Greeley, A. D., Kanekal, S. G., Sibeck, D. G., Schiller, Q., and Baker, D. N. (2021). Evolution of Pitch Angle Distributions of Relativistic Electrons during Geomagnetic Storms: Van Allen Probes Observations. *J. Geophys. Res. Space Phys.* 126, e2020JA028335. doi:10.1029/2020ja028335

Green, J. C., and Kivelson, M. G. (2004). Relativistic Electrons in the Outer Radiation Belt: Differentiating between Acceleration Mechanisms. *J. Geophys. Res.* 109, A03213. doi:10.1029/2003JA010153

Green, J. C. (2006). "Using Electron Phase Space Density Signatures to Identify the Electromagnetic Waves Responsible for Accelerating Relativistic Electrons in Earth's Magnetosphere," in *Magnetospheric ULF Waves: Synthesis and New Directions*. Editors K. Takahashi, P. J. Chi, R. E. Denton, and R. L. Lysak, 225–237. doi:10.1029/169GM15

Hajra, R., Tsurutani, B. T., Echer, E., Gonzalez, W. D., and Santolik, O. (2015). RELATIVISTIC (E> 0.6, > 2.0, AND > 4.0 MeV) ELECTRON ACCELERATION AT GEOSYNCHRONOUS ORBIT DURING HIGH-INTENSITY, LONG-DURATION, CONTINUOUS AE ACTIVITY (HILDCAA) EVENTS. *ApJ* 799, 39. doi:10.1088/0004-637X/799/1/39

Han, S., Murakami, G., Kita, H., Tsuchiya, F., Tao, C., Misawa, H., et al. (2018). Investigating Solar Wind-Driven Electric Field Influence on Long-Term Dynamics of Jovian Synchrotron Radiation. *J. Geophys. Res. Space Phys.* 123, 9508–9516. doi:10.1029/2018JA025849

Hao, Y.-X., Sun, Y.-X., Roussos, E., Liu, Y., Kollmann, P., Yuan, C.-J., et al. (2020). The Formation of Saturn's and Jupiter's Electron Radiation Belts by Magnetospheric Electric Fields. *ApJ* 905, L10. doi:10.3847/2041-8213/abca3f

Hao, Y. X., Zong, Q. G., Zhou, X. Z., Rankin, R., Chen, X. R., Liu, Y., et al. (2019). Global-Scale ULF Waves Associated with SSC Accelerate Magnetospheric Ultrarelativistic Electrons. *J. Geophys. Res. Space Phys.* 124, 1525–1538. doi:10.1029/2018JA026134

Hartinger, M. D., Claudepierre, S. G., Turner, D. L., Reeves, G. D., Breneman, A., Mann, I. R., et al. (2018). Diagnosis of ULF Wave-Particle Interactions with Megaelectron Volt Electrons: The Importance of Ultrahigh-Resolution Energy Channels. *Geophys. Res. Lett.* 45 (11), 883–11,892. doi:10.1029/2018GL080291

Hiraga, R., and Omura, Y. (2020). Acceleration Mechanism of Radiation Belt Electrons through Interaction with Multi-Subpacket Chorus Waves. *Earth Planets Space* 72, 21. doi:10.1186/s40623-020-1134-3

Horne, R. B., Glauert, S. A., Meredith, N. P., Boscher, D., Maget, V., Heynderickx, D., et al. (2013). Space Weather Impacts on Satellites and Forecasting the Earth's Electron Radiation Belts with SPACECAST. *Space weather.* 11, 169–186. doi:10.1002/swe.20023

Horne, R. B., and Thorne, R. M. (1998). Potential Waves for Relativistic Electron Scattering and Stochastic Acceleration during Magnetic Storms. *Geophys. Res. Lett.* 25 (15), 3011–3014. doi:10.1029/98GL01002

Horne, R. B., Thorne, R. M., Shprits, Y. Y., Meredith, N. P., Glauert, S. A., Smith, A. J., et al. (2005). Wave Acceleration of Electrons in the Van Allen Radiation Belts. *Nature* 437, 227–230. doi:10.1038/nature03939

Horne, R., and Tsurutani, B. (2019). Richard Mansergh Thorne (1942-2019). *Eos* 100. (Published on December 04, 2019). doi:10.1029/2019EO137322

Hudson, M., Jaynes, A., Kress, B., Li, Z., Patel, M., Shen, X. C., et al. (2017). Simulated Prompt Acceleration of Multi-MeV Electrons by the 17 March 2015 Interplanetary Shock. *J. Geophys. Res. Space Phys.* 122 (10), 10,036. doi:10.1002/2017JA024445

Hudson, M. K., Elkington, S. R., Li, Z., and Patel, M. (2020). Drift Echoes and Flux Oscillations: A Signature of Prompt and Diffusive Changes in the Radiation Belts. *J. Atmos. Solar-Terrestrial Phys.* 2072020 (105332), 105332–106826. doi:10.1016/j.jastp.2020.105332

Hudson, M. K., Elkington, S. R., Lyon, J. G., Marchenko, V. A., Roth, I., Temerin, M., et al. (1997). Simulations of Radiation Belt Formation during Storm Sudden Commencements. *J. Geophys. Res.* 102 (A7), 14087–14102. doi:10.1029/97JA03995

Hudson, M. K., Kress, B. T., Mueller, H.-R., Zastrow, J. A., and Bernard Blake, J. (2008). Relationship of the Van Allen Radiation Belts to Solar Wind Drivers. *J. Atmos. Solar-Terrestrial Phys.* 70 (5), 708–729. doi:10.1016/j.jastp.2007.11.003

Iles, R. H. A., Meredith, N. P., Fazakerley, A. N., and Horne, R. B. (2006). Phase Space Density Analysis of the Outer Radiation Belt Energetic Electron Dynamics. *J. Geophys. Res.* 111, A03204. doi:10.1029/2005JA011206

Jacobs, J. A. (1970). *Geomagnetic Micropulsations. Physics and Chemistry in Space*, Vol. 1. Berlin, Heidelberg: Springer, 15–63. doi:10.1007/978-3-642-86828-3_2The Morphology of Geomagnetic Micropulsations

Jaynes, A. N., Ali, A. F., Elkington, S. R., Malaspina, D. M., Baker, D. N., Li, X., et al. (2018). Fast Diffusion of Ultrarelativistic Electrons in the Outer Radiation Belt: 17 March 2015 Storm Event. *Geophys Res. Lett.* 45, 10,874–10882. doi:10.1029/2018GL079786

Jaynes, A. N., Baker, D. N., Singer, H. J., Rodriguez, J. V., Loto'aniu, T. M., Ali, A. F., et al. (2015). Source and Seed Populations for Relativistic Electrons: Their Roles in Radiation Belt Changes. *J. Geophys. Res. Space Phys.* 120, 7240–7254. doi:10.1002/2015JA021234

Jaynes, A. N., Li, X., Schiller, Q. G., Blum, L. W., Tu, W., Turner, D. L., Ni, B., Bortnik, J., Baker, D. N., Kanekal, S. G., Blake, J. B., and Wygant, J. (2014). Evolution of Relativistic Outer Belt Electrons during an Extended Quiescent Period. *J. Geophys. Res. Space Phys.* 119 (12), 9558–9566. doi:10.1002/2014ja020125

Jones, S. L., Lessard, M. R., Rychert, K., Spanswick, E., Donovan, E., and Jaynes, A. N. (2013). Persistent, Widespread Pulsating Aurora: A Case Study. *J. Geophys. Res. Space Phys.* 118 (6), 2998–3006. doi:10.1002/jgra.50301

Jordanova, V. K., Tu, W., Chen, Y., Morley, S. K., Panaitescu, A. D., Reeves, G. D., et al. (2016). RAM-SCB Simulations of Electron Transport and Plasma Wave Scattering during the October 2012 "double-dip" Storm. *J. Geophys. Res. Space Phys.* 121, 8712–8727. doi:10.1002/2016JA022470

Kanekal, S. G. (2006). "A Review of Recent Observations of Relativistic Electron Energization in the Earth's Outer Van Allen Radiation Belt (2006)," in *Proceedings of the ILWS Workshop*. Editors N. Gopalswamy and A. Bhattacharyya (Goa, India, 274. ISBN: 81-87099-40-2.

Kanekal, S. G., Baker, D. N., Blake, J. B., Klecker, B., Mewaldt, R. A., and Mason, G. M. (1999). Magnetospheric Response to Magnetic Cloud (Coronal Mass Ejection) Events: Relativistic Electron Observations from SAMPEX and Polar. *J. Geophys. Res.* 104 (A11), 24885–24894. doi:10.1029/1999ja900239

Kanekal, S. G., Baker, D. N., and Blake, J. B. (2001). Multisatellite Measurements of Relativistic Electrons: Global Coherence. *J. Geophys. Res.* 106 (A12), 29721–29732. doi:10.1029/2001JA000070

Katsavrias, C., Aminalragia-Giamini, S., Papadimitriou, C., Daglis, I. A., Sandberg, I., and Jiggens, P. (2022a). *Radiation Belt Model Including Semi-annual Variation and Solar Driving*, 20. Sentinel: Space Weather, e2021SW002936. doi:10.1029/2021SW002936

Katsavrias, C., Papadimitriou, C., Aminalragia-Giamini, S., Daglis, I. A., Sandberg, I., and Jiggens, P. (2021b). On the Semi-annual Variation of Relativistic Electrons in the Outer Radiation Belt. *Ann. Geophys.* 39, 413–425. doi:10.5194/angeo-39-413-2021

Kellerman, A. C., and Shprits, Y. Y. (2012). On the Influence of Solar Wind Conditions on the Outer-Electron Radiation Belt. *J. Geophys. Res.* 117, a–n. doi:10.1029/2011JA017253

Kennel, C. F., and Thorne, R. M. (1967). Unstable Growth of Unducted Whistlers Propagating at an Angle to the Geomagnetic Field. *J. Geophys. Res.* 72 (3), 871–878. doi:10.1029/JZ072i003p00871

Kilpua, E. K. J., Hietala, H., Turner, D. L., Koskinen, H. E. J., Pulkkinen, T. I., Rodriguez, J. V., et al. (2015). Unraveling the Drivers of the Storm Time Radiation Belt Response. *Geophys. Res. Lett.* 42, 3076–3084. doi:10.1002/2015GL063542

Kim, H.-J., and Chan, A. A. (1997). Fully Adiabatic Changes in Storm Time Relativistic Electron Fluxes. *J. Geophys. Res.* 102 (A10), 22107–22116. doi:10.1029/97JA01814

Koller, J., Chen, Y., Reeves, G. D., Friedel, R. H. W., Cayton, T. E., and Vrugt, J. A. (2007). Identifying the Radiation Belt Source Region by Data Assimilation. *J. Geophys. Res.* 112, a–n. doi:10.1029/2006JA012196

Kollmann, P., Roussos, E., Paranicas, C., Krupp, N., Jackman, C. M., Kirsch, E., et al. (2011). Energetic Particle Phase Space Densities at Saturn: Cassini Observations and Interpretations. *J. Geophys. Res.* 116, A05222. doi:10.1029/2010JA016221

Kollmann, P., Roussos, E., Paranicas, C., Woodfield, E. E., Mauk, B. H., Clark, G., et al. (2018). Electron Acceleration to MeV Energies at Jupiter and Saturn. *J. Geophys. Res. Space Phys.* 123, 9110–9129. doi:10.1029/2018JA025665

Koskinen, H. E. J., and Kilpua, E. K. J. (2022). *Physics of Earth's Radiation Belts, Theory and Observations*. Switzerland: Astronomy and Astrophysics Library, Springer. doi:10.1007/978-3-030-82167-8

Kress, B. T., Hudson, M. K., Looper, M. D., Albert, J., Lyon, J. G., and Goodrich, C. C. (2007). Global MHD Test Particle Simulations of >10 MeV Radiation Belt Electrons during Storm Sudden Commencement. *J. Geophys. Res.* 112, a–n. doi:10.1029/2006JA012218

Kress, B. T., Hudson, M. K., Ukhorskiy, A. Y., and Mueller, H.-R. (2012). "Nonlinear Radial Transport in the Earth's Radiation Belts," in *Dynamics of the Earth's Radiation Belts and Inner Magnetosphere, Geophys*. Editor D. Summers (Washington, D. C: Monogr. Ser), 199, 151–160. doi:10.1029/2012GM001333

Kubota, Y., and Omura, Y. (2018). Nonlinear Dynamics of Radiation Belt Electrons Interacting with Chorus Emissions Localized in Longitude. *J. Geophys. Res. Space Phys.* 123, 4835–4857. doi:10.1029/2017JA025050

Lanzerotti, L. J., Roberts, C. S., and Brown, W. L. (1967). Temporal Variations in the Electron Flux at Synchronous Altitudes. *J. Geophys. Res.* 72 (23), 5893–5902. doi:10.1029/JZ072i023p05893

Lejosne, S. (2020). Electromagnetic Radial Diffusion in the Earth's Radiation Belts as Determined by the Solar Wind Immediate Time History and a Toy Model for the Electromagnetic Fields. *JGR Space Phys.* 125, e2020JA027893. doi:10.1029/2020JA027893

Lejosne, S., Fedrizzi, M., Maruyama, N., and Selesnick, R. S. (2021). Thermospheric Neutral Winds as the Cause of Drift Shell Distortion in Earth's Inner Radiation Belt. *Front. Astron. Space Sci.* 8. doi:10.3389/fspas.2021.725800

Lejosne, S., and Kollmann, P. (2020). Radiation Belt Radial Diffusion at Earth and beyond. *Space Sci. Rev.* 216, 19. doi:10.1007/s11214-020-0642-6

Lejosne, S., and Mozer, F. S. (2020). Inversion of the Energetic Electron "Zebra Stripe" Pattern Present in the Earth's Inner Belt and Slot Region: First Observations and Interpretation. *Geophys. Res. Lett.* 47, e2020GL088564. doi:10.1029/2020GL088564

Li, L., Zhou, X. Z., Zong, Q. G., Rankin, R., Zou, H., Liu, Y., et al. (2017). Charged Particle Behavior in Localized Ultralow Frequency Waves: Theory and Observations. *Geophys. Res. Lett.* 44, 5900–5908. doi:10.1002/2017GL073392

Li, W., and Hudson, M. K. (2019). Earth's Van Allen Radiation Belts: From Discovery to the Van Allen Probes Era. *J. Geophys. Res. Space Phys.* 124, 8319–8351. doi:10.1029/2018JA025940

Li, W., Shprits, Y. Y., and Thorne, R. M. (2007). Dynamic Evolution of Energetic Outer Zone Electrons Due to Wave-Particle Interactions during Storms. *J. Geophys. Res.* 112 (A10), a–n. doi:10.1029/2007JA012368

Li, X., Baker, D. N., Temerin, M., Larson, D., Lin, R. P., Reeves, G. D., et al. (1997). Are Energetic Electrons in the Solar Wind the Source of the Outer Radiation Belt? *Geophys. Res. Lett.* 24 (8), 923–926. doi:10.1029/97GL00543

Li, X., Baker, D. N., Temerin, M., Reeves, G., Friedel, R., and Shen, C. (2005). Energetic Electrons, 50 keV to 6 MeV, at Geosynchronous Orbit: Their Responses to Solar Wind Variations. *Space weather.* 3, a–n. doi:10.1029/2004SW000105

Li, X., Roth, I., Temerin, M., Wygant, J. R., Hudson, M. K., and Blake, J. B. (1993). Simulation of the Prompt Energization and Transport of Radiation Belt Particles during the March 24, 1991 SSC. *Geophys. Res. Lett.* 20 (22), 2423–2426. doi:10.1029/93gl02701

Li, X., Temerin, M., Baker, D. N., and Reeves, G. D. (2011). Behavior of MeV Electrons at Geosynchronous Orbit during Last Two Solar Cycles. *J. Geophys. Res.* 116, a–n. doi:10.1029/2011JA016934

Li, X., Temerin, M., Baker, D. N., Reeves, G. D., and Larson, D. (2001). Quantitative Prediction of Radiation Belt Electrons at Geostationary Orbit Based on Solar Wind Measurements. *Geophys. Res. Lett.* 28 (9), 1887–1890. doi:10.1029/2000GL012681

Li, Z., Hudson, M., Patel, M., Wiltberger, M., Boyd, A., and Turner, D. (2017). ULF Wave Analysis and Radial Diffusion Calculation Using a Global MHD Model for the 17 March 2013 and 2015 Storms. *J. Geophys. Res. Space Phys.* 122, 7353–7363. doi:10.1002/2016JA023846

Liu, W., Tu, W., Li, X., Sarris, T., Khotyaintsev, Y., Fu, H., et al. (2016). On the Calculation of Electric Diffusion Coefficient of Radiation Belt Electrons with *In Situ* Electric Field Measurements by THEMIS. *Geophys. Res. Lett.* 43, 1023–1030. doi:10.1002/2015GL067398

Loridan, V., Ripoll, J.-F., Tu, W., and Cunningham, G. S. (2019). On the Use of Different Magnetic Field Models for Simulating the Dynamics of the Outer Radiation Belt Electrons During the October 1990 Storm. *J. Geophys. Res. Space Phys.* 124, 6453–6486. doi:10.1029/2018JA026392

Louarn, P., Kivelson, M. G., and Kurth, W. S. (2016). On the Links between the Radio Flux and Magnetodisk Distortions at Jupiter. *J. Geophys. Res. Space Phys.* 121, 9651–9670. doi:10.1002/2016JA023106

Louarn, P., Paranicas, C. P., and Kurth, W. S. (2014). Global Magnetodisk Disturbances and Energetic Particle Injections at Jupiter. *J. Geophys. Res. Space Phys.* 119, 4495–4511. doi:10.1002/2014JA019846

Lukin, A. S., Artemyev, A. V., and Petrukovich, A. A. (2021). On Application of Stochastic Differential Equations for Simulation of Nonlinear Wave-Particle Resonant Interactions. *Phys. Plasmas* 28, 092904. doi:10.1063/5.0058054

Lyon, J., Fedder, J., and Mobarry, C. (2004). The Lyon–Fedder–Mobarry (LFM) Global MHD Magnetospheric Simulation Code. *J. Atmos.*

Ma, Q., Li, W., Bortnik, J., Thorne, R. M., Chu, X., Ozeke, L. G., et al. (2018). Quantitative Evaluation of Radial Diffusion and Local Acceleration Processes during GEM Challenge Events. *J. Geophys. Res. Space Phys.* 123, 1938–1952. doi:10.1002/2017JA025114

Malaspina, D. M., Jaynes, A. N., Boulé, C., Bortnik, J., Thaller, S. A., Ergun, R. E., et al. (2016). The Distribution of Plasmaspheric Hiss Wave Power with Respect to Plasmapause Location. *Geophys. Res. Lett.* 43, 7878–7886. doi:10.1002/2016GL069982

Malaspina, D. M., Zhu, H., and Drozdov, A. Y. (2020). A Wave Model and Diffusion Coefficients for Plasmaspheric Hiss Parameterized by Plasmapause Location. *J. Geophys. Res. Space Phys.* 125, e2019JA027415. doi:10.1029/2019JA027415

Mauk, B. H., Saur, J., Mitchell, D. G., Roelof, E. C., Brandt, P. C., Armstrong, T. P., et al. (2005). Energetic Particle Injections in Saturn's Magnetosphere. *Geophys. Res. Lett.* 32, a–n. doi:10.1029/2005GL022485

McIlwain, C. E. (1961). Coordinates for Mapping the Distribution of Magnetically Trapped Particles. *J. Geophys. Res.* 66 (11), 3681–3691. doi:10.1029/JZ066i011p03681

McPherron, R. L., Baker, D. N., and Crooker, N. U. N. U. (2009). Role of the Russell-McPherron Effect in the Acceleration of Relativistic Electrons. *J. Atmos. Solar-Terrestrial Phys.* 71 (10–11), 1032–1044. doi:10.1016/j.jastp.2008.11.002

Meredith, N. P., Cain, M., Horne, R. B., Thorne, R. M., Summers, D., and Anderson, R. R. (2003). Evidence for Chorus-Driven Electron Acceleration to Relativistic Energies from a Survey of Geomagnetically Disturbed Periods. *J. Geophys. Res.* 108, 1248. doi:10.1029/2002JA009764

Meredith, N. P., Horne, R. B., Iles, R. H. A., Thorne, R. M., Heynderickx, D., and Anderson, R. R. (2002). Outer Zone Relativistic Electron Acceleration Associated with Substorm-Enhanced Whistler Mode Chorus. *J. Geophys. Res.* 107 (A7). doi:10.1029/2001JA900146

Mihalov, J. D., Fischer, H. M., Pehlke, E., and Lanzerotti, L. J. (2000). Energetic Trapped Electron Measurements from the Galileo Jupiter Probe. *Geophys. Res. Lett.* 27, 2445–2448. doi:10.1029/2000GL003812

Miyoshi, Y., and Kataoka, R. (2008). Flux Enhancement of the Outer Radiation Belt Electrons after the Arrival of Stream Interaction Regions. *J. Geophys. Res.* 113, a–n. doi:10.1029/2007JA012506

Miyoshi, Y., Misawa, H., Morioka, A., Kondo, T., Koyama, Y., and Nakajima, J. (1999). Observation of Short-Term Variation of Jupiter's Synchrotron Radiation. *Geophys. Res. Lett.* 26, 9–12. doi:10.1029/1998GL900244

Miyoshi, Y., Morioka, A., Obara, T., Misawa, H., Nagai, T., and Kasahara, Y. (2003). Rebuilding Process of the Outer Radiation Belt during the 3 November 1993 Magnetic Storm: NOAA and Exos-D Observations. *J. Geophys. Res.* 108 (A1), 1004. doi:10.1029/2001JA007542

Miyoshi, Y., Saito, S., Kurita, S., Asamura, K., Hosokawa, K., Sakanoi, T., and Blake, J. B. (2020). Relativistic Electron Microbursts as High-energy Tail of Pulsating Aurora Electrons. *Geophys. Res. Lett.* 47 (21), e2020GL090360. doi:10.1029/2020gl090360

Moya, P. S., Pinto, V. A., Sibeck, D. G., Kanekal, S. G., and Baker, D. N. (2017). On the Effect of Geomagnetic Storms on Relativistic Electrons in the Outer Radiation Belt: Van Allen Probes Observations. *J. Geophys. Res. Space Phys.* 122, 11,100–11,108. doi:10.1002/2017JA024735

Mozer, F. S., Agapitov, O. V., Artemyev, A., Drake, J. F., Krasnoselskikh, V., Lejosne, S., et al. (2015). Time Domain Structures: What and where They Are, what They Do, and How They Are Made. *Geophys. Res. Lett.* 42, 3627–3638. doi:10.1002/10.1002/2015gl063946

Mozer, F. S., Artemyev, A., Agapitov, O. V., Mourenas, D., and Vasko, I. (2016). Near-relativistic Electron Acceleration by Landau Trapping in Time Domain Structures. *Geophys. Res. Lett.* 43, 508–514. doi:10.1002/2015GL067316

Murakami, G., Yoshioka, K., Yamazaki, A., Tsuchiya, F., Kimura, T., Tao, C., et al. (2016). Response of Jupiter's Inner Magnetosphere to the Solar Wind Derived from Extreme Ultraviolet Monitoring of the Io Plasma Torus. *Geophys. Res. Lett.* 43 (12), 308. doi:10.1002/2016GL071675

Nénon, Q., Sicard, A., and Bourdarie, S. (2017). A New Physical Model of the Electron Radiation Belts of Jupiter inside Europa's Orbit. *J. Geophys. Res. Space Phys.* 122, 5148–5167. doi:10.1002/2017JA023893

Northrop, T. G. (1963). *The Adiabatic Motion of Charged Particles*. New York: Wiley-Interscience. 978-0470651391.

Nunn, D., Demekhov, A., Trakhtengerts, V., and Rycroft, M. J. (2003). VLF Emission Triggering by a Highly Anisotropic Energetic Electron Plasma. *Ann. Geophys.* 21, 481–492. doi:10.5194/angeo-21-481-2003

O'Brien, T. P. (2014). Breaking All the Invariants: Anomalous Electron Radiation Belt Diffusion by Pitch Angle Scattering in the Presence of Split Magnetic Drift Shells. *Geophys. Res. Lett.* 41, 216–222. doi:10.1002/2013GL058712

O'Brien, T. P., Lorentzen, K. R., Mann, I. R., Meredith, N. P., Blake, J. B., Fennell, J. F., et al. (2003). Energization of Relativistic Electrons in the Presence of ULF Power and MeV Microbursts: Evidence for Dual ULF and VLF Acceleration. *J. Geophys. Res.* 108, 1329. doi:10.1029/2002JA009784

Olifer, L., Mann, I. R., Morley, S. K., Ozeke, L. G., and Choi, D. (2018). On the Role of Last Closed Drift Shell Dynamics in Driving Fast Losses and Van Allen Radiation Belt Extinction. *J. Geophys. Res. Space Phys.* 123, 3692–3703. doi:10.1029/2018JA025190

Olifer, L., Mann, I. R., Ozeke, L. G., Morley, S. K., and Louis, H. L. (2021). On the Formation of Phantom Electron Phase Space Density Peaks in Single Spacecraft Radiation Belt Data. *Geophys. Res. Lett.* 48, e2020GL092351. doi:10.1029/2020GL092351

Omura, Y., Furuya, N., and Summers, D. (2007). Relativistic Turning Acceleration of Resonant Electrons by Coherent Whistler Mode Waves in a Dipole Magnetic Field. *J. Geophys. Res.* 112, a–n. doi:10.1029/2006JA012243

Omura, Y., Miyashita, Y., Yoshikawa, M., Summers, D., Hikishima, M., Ebihara, Y., et al. (2015). Formation Process of Relativistic Electron Flux through Interaction with Chorus Emissions in the Earth's Inner Magnetosphere. *J. Geophys. Res. Space Phys.* 120, 9545–9562. doi:10.1002/2015JA021563

Omura, Y. (2021). Nonlinear Wave Growth Theory of Whistler-Mode Chorus and Hiss Emissions in the Magnetosphere. *Earth Planets Space* 73, 95. doi:10.1186/s40623-021-01380-w

Omura, Y., and Summers, D. (2004). Computer Simulations of Relativistic Whistler-Mode Wave-Particle Interactions. *Phys. Plasmas* 11 (7), 3530–3534. doi:10.1063/1.1757457

Orlova, K., Shprits, Y., and Spasojevic, M. (2016). New Global Loss Model of Energetic and Relativistic Electrons Based on Van Allen Probes Measurements. *J. Geophys. Res. Space Phys.* 121, 1308–1314. doi:10.1002/2015JA021878

Orlova, K., Spasojevic, M., and Shprits, Y. (2014). Activity-dependent Global Model of Electron Loss inside the Plasmasphere. *Geophys. Res. Lett.* 41, 3744–3751. doi:10.1002/2014GL060100

Ozeke, L. G., Mann, I. R., Claudepierre, S. G., Henderson, M., Morley, S. K., and Murphy, K. R. (2019). The March 2015 Superstorm Revisited: Phase Space Density Profiles and Fast ULF Wave Diffusive Transport. *J. Geophys. Res. Space Phys.* 124, 1143–1156. doi:10.1029/2018JA026326

Ozeke, L. G., Mann, I. R., Dufresne, S. K. Y., Olifer, L., Morley, S. K., Claudepierre, S. G., et al. (2020). Rapid Outer Radiation Belt Flux Dropouts and Fast Acceleration during the March 2015 and 2013 Storms: The Role of ULF Wave Transport from a Dynamic Outer Boundary. *J. Geophys. Res. Space Phys.* 125, e2019JA027179. doi:10.1029/2019JA027179

Ozeke, L. G., Mann, I. R., Murphy, K. R., Jonathan Rae, I., and Milling, D. K. (2014a). Analytic Expressions for ULF Wave Radiation Belt Radial Diffusion Coefficients. *J. Geophys. Res. Space Phys.* 119, 1587–1605. doi:10.1002/2013JA019204

Ozeke, L. G., Mann, I. R., Olifer, L., Claudepierre, S. G., Spence, H. E., and Baker, D. N. (2022). Statistical Characteristics of Energetic Electron Pitch Angle Distributions in the Van Allen Probe Era: 1. Butterfly Distributions with Flux Peaks at Preferred Pitch Angles. *J. Geophys. Res. Space Phys.* 127, e2021JA029907. doi:10.1029/2021JA029907

Ozeke, L. G., Mann, I. R., Turner, D. L., Murphy, K. R., Degeling, A. W., Rae, I. J., et al. (2014b). Modeling Cross L Shell Impacts of Magnetopause Shadowing and ULF Wave Radial Diffusion in the Van Allen Belts. *Geophys. Res. Lett.* 41, 6556–6562. doi:10.1002/2014GL060787

Palmaerts, B., Roussos, E., Krupp, N., Kurth, W. S., Mitchell, D. G., and Yates, J. N. (2016). Statistical Analysis and Multi-Instrument Overview of the Quasi-Periodic 1-hour Pulsations in Saturn's Outer Magnetosphere. *Icarus* 271, 1. doi:10.1016/j.icarus.2016.01.025

Paranicas, C., Thomsen, M. F., Kollmann, P., Azari, A. R., Bader, A., Badman, S. V., et al. (2020). Inflow Speed Analysis of Interchange Injections in Saturn's Magnetosphere. *J. Geophys. Res. (Space Phys.* 125, e28299. doi:10.1029/2020JA028299

Paulikas, G. A., and Blake, J. B. (1979). "Effects of the Solar Wind on Magnetospheric Dynamics: Energetic Electrons at the Synchronous Orbit," in *Quantitative Modeling of Magnetospheric Processes*. Editor W. P. Olson (Washington, D. C: Geophys. Monogr. Ser.AGU), 21, 180–202.

Reeves, G. D., McAdams, K. L., Friedel, R. H. W., and O'Brien, T. P. (2003). Acceleration and Loss of Relativistic Electrons during Geomagnetic Storms. *Geophys. Res. Lett.* 30, 1529. doi:10.1029/2002GL016513

Reeves, G. D., Morley, S. K., Friedel, R. H. W., Henderson, M. G., Cayton, T. E., Cunningham, G., et al. (2011). On the Relationship between Relativistic Electron Flux and Solar Wind Velocity: Paulikas and Blake Revisited. *J. Geophys. Res.* 116, A02213. doi:10.1029/2010JA015735

Reeves, G. D., Spence, H. E., Henderson, M. G., Morley, S. K., Friedel, R. H. W., Funsten, H. O., et al. (2013). Electron Acceleration in the Heart of the Van Allen Radiation Belts. *Science* 341 (6149), 991–994. doi:10.1126/science.1237743

Riley, P., and Wolf, R. A. (1992). Comparison of Diffusion and Particle Drift Descriptions of Radial Transport in the Earth's Inner Magnetosphere. *J. Geophys. Res.* 97 (A11), 16865–16876. doi:10.1029/92JA01538

Ripoll, J-F. (2020). Particle Dynamics in the Earth's Radiation Belts: Review of Current Research and Open Questions. *J. Geophys. Res. Space Phys.* 125, 5e2019JA026735. doi:10.1029/2019ja026735

Ripoll, J.-F., Loridan, V., Denton, M. H., Cunningham, G., Reeves, G., Santolík, O., et al. (2019). Observations and Fokker-Planck Simulations of the L-Shell, Energy, and Pitch Angle Structure of Earth's Electron Radiation Belts during Quiet Times. *J. Geophys. Res. Space Phys.* 124, 1125–1142. doi:10.1029/2018JA026111

Rodger, C. J., Hendry, A. T., Clilverd, M. A., Forsyth, C., and Morley, S. K. (2022). Examination of Radiation Belt Dynamics during Substorm Clusters: Activity Drivers and Dependencies of Trapped Flux Enhancements. *J. Geophys. Res. Space Phys.* 127, e2021JA030003. doi:10.1029/2021JA030003

Roederer, J. G. (1970). *Dynamics of Geomagnetically Trapped Radiation*. New York: Springer. doi:10.1007/978-3-642-49300-3

Roederer, J. G., and Lejosne, S. (2018). Coordinates for Representing Radiation Belt Particle Flux. *J. Geophys. Res. Space Phys.* 123, 1381–1387. doi:10.1002/2017JA025053

Roederer, J. G., and Zhang, H. (2014). "Dynamics of Magnetically Trapped Particles," in *Foundations of the Physics of Radiation Belts and Space Plasmas. Astrophysics and Space Science Library* (Berlin: Springer), 403. doi:10.1007/978-3-642-41530-2

Roussos, E., Allanson, O., André, N., Bertucci, B., Branduardi-Raymont, G., Clark, G., et al. (2021). The Iin-Ssitu Exploration of Jupiter's Radiation Belts. *Exp. Astron.* doi:10.1007/s10686-021-09801-0

Roussos, E., Jackman, C. M., Thomsen, M. F., Kurth, W. S., Badman, S. V., Paranicas, C., et al. (2018b). Solar Energetic Particles (SEP) and Galactic Cosmic Rays (GCR) as Tracers of Solar Wind Conditions Near Saturn: Event Lists and Applications. *Icarus* 300, 47. doi:10.1016/j.icarus.2017.08.040

Roussos, E., Jones, G. H., Krupp, N., Paranicas, C., Mitchell, D. G., Lagg, A., et al. (2007). Electron Microdiffusion in the Saturnian Radiation Belts: Cassini MIMI/LEMMS Observations of Energetic Electron Absorption by the Icy Moons. *J. Geophys. Res. (Space Phys.* 112, A06214. doi:10.1029/2006JA012027

Roussos, E., Kollmann, P., Krupp, N., Paranicas, C., Dialynas, K., Sergis, N., et al. (2018a). Drift-resonant, Relativistic Electron Acceleration at the Outer Planets: Insights from the Response of Saturn's Radiation Belts to Magnetospheric Storms. *Icarus* 305, 160. doi:10.1016/j.icarus.2018.01.016

Roussos, E., and Kollmann, P. (2021). The Radiation Belts of Jupiter and Saturn. *Magnetos. Sol. Syst.* 2, 499. doi:10.1002/9781119815624.ch32

Roussos, E., Krupp, N., Mitchell, D. G., Paranicas, C., Krimigis, S. M., Andriopoulou, M., et al. (2016). Quasi-periodic Injections of Relativistic Electrons in Saturn's Outer Magnetosphere. *Icarus* 263, 101. doi:10.1016/j.icarus.2015.04.017

Roussos, E., Krupp, N., Paranicas, C. P., Mitchell, D. G., Müller, A. L., Kollmann, P., et al. (2010). Energetic Electron Microsignatures as Tracers of Radial Flows and Dynamics in Saturn's Innermost Magnetosphere. *J. Geophys. Res. (Space Phys.* 115, A03202. doi:10.1029/2009JA014808

Sandhu, J. K., Rae, I. J., Wygant, J. R., Breneman, A. W., Tian, S., Watt, C. E. J., et al. (2021). ULF Wave Driven Radial Diffusion during Geomagnetic Storms: A Statistical Analysis of Van Allen Probes Observations. *J. Geophys. Res. Space Phys.* 126, e2020JA029024. doi:10.1029/2020JA029024

Schiller, Q., Kanekal, S. G., Jian, L. K., Li, X., Jones, A., Baker, D. N., et al. (2016). *Prompt Injections of Highly Relativistic Electrons Induced by Interplanetary Shocks: A Statistical Study of Van Allen Probes Observations*.

Schiller, Q., Li, X., Blum, L., Tu, W., Turner, D. L., and Blake, J. B. (2014). A Nonstorm Time Enhancement of Relativistic Electrons in the Outer Radiation Belt. *Geophys. Res. Lett.* 41, 7–12. doi:10.1002/2013GL058485

Schulz, M. (1972). Drift-Shell Splitting at Arbitrary Pitch Angle. *J. Geophys. Res.* 77, 624–634. doi:10.1029/JA077i004p00624

Schulz, M., and Lanzerotti, L. J. (1974). *Particle Diffusion in the Radiation Belts*. Berlin: Springer. doi:10.1007/978-3-642-65675-0

Selesnick, R. S., Blake, J. B., Kolasinski, W. A., and Fritz, T. A. (1997). A Quiescent State of 3 to 8 MeV Radiation Belt Electrons. *Geophys. Res. Lett.* 24 (11), 1343–1346. doi:10.1029/97GL51407

Selesnick, R. S., and Blake, J. B. (2000). On the Source Location of Radiation Belt Relativistic Electrons. *J. Geophys. Res.* 105 (A2), 2607–2624. doi:10.1029/1999JA900445

Selesnick, R. S., and Stone, E. C. (1991). Energetic Electrons at Uranus: Bimodal Diffusion in a Satellite Limited Radiation Belt. *J. Geophys. Res.* 96, 5651. doi:10.1029/90JA02696

Selesnick, R. S., Su, Y.-J., and Blake, J. B. (2016). Control of the Innermost Electron Radiation Belt by Large-Scale Electric Fields. *J. Geophys. Res. Space Phys.* 121, 8417–8427. doi:10.1002/2016JA022973

Shprits, Y., Kondrashov, D., Chen, Y., Thorne, R., Ghil, M., Friedel, R., et al. (2007a). Reanalysis of Relativistic Radiation Belt Electron Fluxes Using CRRES Satellite Data, a Radial Diffusion Model, and a Kalman Filter. *J. Geophys. Res.* 112, A12216. doi:10.1029/2007JA012579

Shprits, Y. Y., Kellerman, A. C., Drozdov, A. Y., Spence, H. E., Reeves, G. D., and Baker, D. N. (2015). Combined Convective and Diffusive Simulations: VERB-4D Comparison with 17 March 2013 Van Allen Probes Observations. *Geophys. Res. Lett.* 42, 9600–9608. doi:10.1002/2015GL065230

Shprits, Y. Y., Menietti, J. D., Gu, X., Kim, K. C., and Horne, R. B. (2012). Gyroresonant Interactions between the Radiation Belt Electrons and Whistler Mode Chorus Waves in the Radiation Environments of Earth, Jupiter, and Saturn: A Comparative Study. *J. Geophys. Res. (Space Phys.* 117, A11216. doi:10.1029/2012JA018031

Shprits, Y. Y., Meredith, N. P., and Thorne, R. M. (2007b). Parameterization of Radiation Belt Electron Loss Timescales Due to Interactions with Chorus Waves. *Geophys. Res. Lett.* 34 (11). doi:10.1029/2006gl029050

Shprits, Y. Y., Subbotin, D. A., Meredith, N. P., and Elkington, S. R. (2008). Review of Modeling of Losses and Sources of Relativistic Electrons in the Outer Radiation Belt II: Local Acceleration and Loss. *J. Atmos. Solar-Terrestrial Phys.* 70 (14), 1694–1713. doi:10.1016/j.jastp.2008.06.014

Shprits, Y. Y., Thorne, R. M., Friedel, R., Reeves, G. D., Fennell, J., Baker, D. N., et al. (2006). Outward Radial Diffusion Driven by Losses at Magnetopause. *J. Geophys. Res.* 111, A11214. doi:10.1029/2006JA011657

Shprits, Y. Y., Thorne, R. M., Reeves, G. D., and Friedel, R. (2005). Radial Diffusion Modeling with Empirical Lifetimes: Comparison with CRRES Observations. *Ann. Geophys.* 23, 1467–1471. doi:10.5194/angeo-23-1467-2005

Shprits, Y. Y., and Thorne, R. M. (2004). Time Dependent Radial Diffusion Modeling of Relativistic Electrons with Realistic Loss Rates. *Geophys. Res. Lett.* 31, L08805. doi:10.1029/2004GL019591

Simms, L. E., Engebretson, M. J., Clilverd, M. A., Rodger, C. J., and Reeves, G. D. (2018). Nonlinear and Synergistic Effects of ULF Pc5, VLF Chorus, and EMIC Waves on Relativistic Electron Flux at Geosynchronous Orbit. *J. Geophys. Res. Space Phys.* 123, 4755–4766. doi:10.1029/2017JA025003

Simms, L. E., Engebretson, M. J., Rodger, C. J., Dimitrakoudis, S., Mann, I. R., and Chi, P. J. (2021). The Combined Influence of Lower Band Chorus and ULF Waves on Radiation Belt Electron Fluxes at Individual L-Shells. *J. Geophys. Res. Space Phys.* 126, e2020JA028755. doi:10.1029/2020JA028755

Staples, F. A., Kellerman, A., Murphy, K. R., Rae, I. J., Sandhu, J. K., and Forsyth, C. (2022). Resolving Magnetopause Shadowing Using Multimission Measurements of Phase Space Density. *J. Geophys. Res. Space Phys.* 127, e2021JA029298. doi:10.1029/2021JA029298

Staples, F. A., Rae, I. J., Forsyth, C., Smith, A. R. A., Murphy, K. R., Raymer, K. M., et al. (2020). Do statistical Models Capture the Dynamics of the Magnetopause during Sudden Magnetospheric Compressions? *J. Geophys. Res. Space Phys.* 125, e2019JA027289. doi:10.1029/2019ja027289

Stern, D. P. (1977). Large-scale Electric Fields in the Earth's Magnetosphere. *Rev. Geophys.* 15 (2), 156–194. doi:10.1029/RG015i002p00156

Su, Z., Zhu, H., Xiao, F., Zong, Q.-G., Zhou, X.-Z., Zhen, H., et al. (2015). Ultra-low-frequency Wave-Driven Diffusion of Radiation Belt Relativistic Electrons. *Nat. Commun.* 6, 10096. doi:10.1038/ncomms10096

Subbotin, D., Shprits, Y., and Ni, B. (2010). Three-dimensional VERB Radiation Belt Simulations Including Mixed Diffusion. *J. Geophys. Res. [Space Phys.* 115 (A3). doi:10.1029/2009JA015070

Summers, D., Ma, C., and Mukai, T. (2004). Competition between Acceleration and Loss Mechanisms of Relativistic Electrons during Geomagnetic Storms. *J. Geophys. Res. Space Phys.* 109 (A4). doi:10.1029/2004ja010437

Summers, D., and Omura, Y. (2007). Ultra-relativistic Acceleration of Electrons in Planetary Magnetospheres. *Geophys. Res. Lett.* 34, L24205. doi:10.1029/2007GL032226

Summers, D., Thorne, R. M., and Xiao, F. (1998). Relativistic Theory of Wave-Particle Resonant Diffusion with Application to Electron Acceleration in the Magnetosphere. *J. Geophys. Res.* 103 (A9), 20487–20500. doi:10.1029/98JA01740

Sun, Y. X., Roussos, E., Hao, Y. X., Zong, Q.-G., Liu, Y., Lejosne, S., et al. (2021). Saturn's Inner Magnetospheric Convection in the View of Zebra Stripe Patterns in Energetic Electron Spectra. *J. Geophys. Res. (Space Phys.* 126, e29600. doi:10.1029/2021JA029600

Sun, Y. X., Roussos, E., Krupp, N., Zong, Q. G., Kollmann, P., and Zhou, X. Z. (2019). Spectral Signatures of Adiabatic Electron Acceleration at Saturn through Corotation Drift Cancelation. *Geophys. Res. Lett.* 46 (10), 240. doi:10.1029/2019GL084113

Tao, X., Bortnik, J., Albert, J. M., and Thorne, R. M. (2012). Comparison of Bounce-Averaged Quasi-Linear Diffusion Coefficients for Parallel Propagating Whistler Mode Waves with Test Particle Simulations. *J. Geophys. Res.* 117, A10205. doi:10.1029/2012JA017931

Thorne, R., Li, W., Ni, B., Ma, Q., Bortnik, J., Chen, L., et al. (2013). Rapid Local Acceleration of Relativistic Radiation-Belt Electrons by Magnetospheric Chorus. *Nature* 504, 411–414. doi:10.1038/nature12889

Thorne, R. M., Armstrong, T. P., Stone, S., Williams, D. J., McEntire, R. W., Bolton, S. J., et al. (1997). Galileo Evidence for Rapid Interchange Transport in the Io Torus. *Geophys. Res. Lett.* 24, 2131. doi:10.1029/97GL01788

Thorne, R. M., Church, S. R., and Gorney, D. J. (1979). On the Origin of Plasmaspheric Hiss: The Importance of Wave Propagation and the Plasmapause. *J. Geophys. Res. Space Phys.* 84 (A9), 5241–5247. doi:10.1029/ja084ia09p05241

Thorne, R. M., Horne, R. B., Glauert, S., Meredith, N. P., Shprits, Y. Y., Summers, D., et al. (2005). The Influence of Wave-Particle Interactions on Relativistic Electron Dynamics during Storms. *Geophys. Monograph-American Geophys. Union* 159, 101. doi:10.1029/159gm07

Thorne, R. M. (2010). Radiation Belt Dynamics: The Importance of Wave-particle Interactions. *Geophys. Res. Lett.* 37, L22107. doi:10.1029/2010GL044990

Tsuchiya, F., Misawa, H., Imai, K., and Morioka, A. (2011). Short-term Changes in Jupiter's Synchrotron Radiation at 325 MHz: Enhanced Radial Diffusion in Jupiter's Radiation Belt Driven by Solar UV/EUV Heating. *J. Geophys. Res. (Space Phys.* 116, A09202. doi:10.1029/2010JA016303

Tsurutani, B. T., Gonzalez, W. D., Gonzalez, A. L. C., Guarnieri, F. L., Gopalswamy, N., Grande, M., et al. (2006). Corotating Solar Wind Streams and Recurrent Geomagnetic Activity: A Review. *J. Geophys. Res.* 111, A07S01. doi:10.1029/2005JA011273

Tu, W., Elkington, S. R., Li, X., Liu, W., and Bonnell, J. (2012). Quantifying Radial Diffusion Coefficients of Radiation Belt Electrons Based on Global MHD Simulation and Spacecraft Measurements. *J. Geophys. Res.* 117, A10210. doi:10.1029/2012JA017901

Tu, W., Li, X., Chen, Y., Reeves, G. D., and Temerin, M. (2009). Storm-dependent Radiation Belt Electron Dynamics. *J. Geophys. Res.* 114, A02217. doi:10.1029/2008JA013480

Turner, D. L., Cohen, I. J., Michael, A., Sorathia, K., Merkin, S., Mauk, B. H., et al. (2021). Can Earth's Magnetotail Plasma Sheet Produce a Source of Relativistic Electrons for the Radiation Belts? *Geophys. Res. Lett.* 48, e2021GL095495. doi:10.1029/2021GL095495

Turner, D. L., Kilpua, E. K. J., Hietala, H., Claudepierre, S. G., O'Brien, T. P., Fennell, J. F., et al. (2019). The Response of Earth's Electron Radiation Belts to Geomagnetic Storms: Statistics from the Van Allen Probes Era Including Effects from Different Storm Drivers. *J. Geophys. Res. Space Phys.* 124, 1013–1034. doi:10.1029/2018JA026066

Turner, D. L., Shprits, Y., Hartinger, M., and Angelopoulos, V. (2012). Explaining Sudden Losses of Outer Radiation Belt Electrons during Geomagnetic Storms. *Nat. Phys.* 8 (3), 208–212. doi:10.1038/nphys2185

Tverskaya, L. V., Pavlov, N. N., Blake, J. B., Selesnick, R. S., and Fennell, J. F. (2003). Predicting the L-Position of the Storm-Injected Relativistic Electron Belt. *Adv. Space Res.* 31 (4), 1039–1044. doi:10.1016/S0273-1177(02)00785-8

Ukhorskiy, A. Y., Anderson, B. J., Brandt, P. C., and Tsyganenko, N. A. (2006). Storm Time Evolution of the Outer Radiation Belt: Transport and Losses. *J. Geophys. Res.* 111, A11S03. doi:10.1029/2006JA011690

Ukhorskiy, A. Y., and Sitnov, M. I. (2012). "Dynamics of Radiation Belt Particles," in *The Van Allen Probes Mission*. Editors N. Fox and J. L. Burch (Boston, MA: Springer). doi:10.1007/978-1-4899-7433-4_17

Ukhorskiy, A. Y., and Sitnov, M. I. (2013). Dynamics of Radiation Belt Particles. *Space Sci. Rev.* 179, 545–578. doi:10.1007/s11214-012-9938-5

Ukhorskiy, A. Y., Sitnov, M. I., Millan, R. M., and Kress, B. T. (2011). The Role of Drift Orbit Bifurcations in Energization and Loss of Electrons in the Outer Radiation Belt. *J. Geophys. Res.* 116, A09208. doi:10.1029/2011JA016623

Ukhorskiy, A. Y., Sitnov, M. I., Takahashi, K., and Anderson, B. J. (2009). Radial Transport of Radiation Belt Electrons Due to Stormtime Pc5 Waves. *Ann. Geophys.* 27, 2173–2181. doi:10.5194/angeo-27-2173-2009

Van Allen, J. A., Thomsen, M. F., and Randall, B. A. (1980). The Energetic Charged Particle Absorption Signature of Mimas. *J. Geophys. Res.* 85, 5709. doi:10.1029/JA085iA11p05709

Varotsou, A., Boscher, D., Bourdarie, S., Horne, R. B., Glauert, S. A., and Meredith, N. P. (2005). Simulation of the Outer Radiation Belt Electrons Near Geosynchronous Orbit Including Both Radial Diffusion and Resonant Interaction with Whistler-Mode Chorus Waves. *Geophys. Res. Lett.* 32, L19106. doi:10.1029/2005GL023282

Walt, M. (1994). *Introduction to Geomagnetically Trapped Radiation*. Cambridge: Cambridge University Press. doi:10.1017/CBO9780511524981

Wang, D., and Shprits, Y. Y. (2019). On How High-Latitude Chorus Waves Tip the Balance between Acceleration and Loss of Relativistic Electrons. *Geophys. Res. Lett.* 46 (14), 7945–7954. doi:10.1029/2019GL082681

Wang, D., Shprits, Y. Y., Zhelavskaya, I. S., Effenberger, F., Castillo, A., Drozdov, A. Y., et al. (2020). The Effect of Plasma Boundaries on the Dynamic Evolution of Relativistic Radiation Belt Electrons. *J. Geophys. Res. Space Phys.* 125, e2019JA027422. doi:10.1029/2019JA027422

Watt, C. E. J., Rae, I. J., Murphy, K. R., Anekallu, C., Bentley, S. N., and Forsyth, C. (2017). The Parameterization of Wave-Particle Interactions in the Outer Radiation Belt. *J. Geophys. Res. Space Phys.* 122, 9545–9551. doi:10.1002/2017JA024339

Williams, D. J. (1966). A 27-day Periodicity in Outer Zone Trapped Electron Intensities. *J. Geophys. Res.* 71 (7), 1815–1826. doi:10.1029/JZ071i007p01815

Wing, S., Johnson, J. R., Camporeale, E., and Reeves, G. D. (2016). Information Theoretical Approach to Discovering Solar Wind Drivers of the Outer Radiation Belt. *J. Geophys. Res. Space Phys.* 121, 9378–9399. doi:10.1002/2016JA022711

Woodfield, E. E., Glauert, S. A., Menietti, J. D., Averkamp, T. F., Horne, R. B., and Shprits, Y. Y. (2019). Rapid Electron Acceleration in Low-Density Regions of Saturn's Radiation Belt by Whistler Mode Chorus Waves. *Geophys. Res. Lett.* 46, 7191. doi:10.1029/2019GL083071

Woodfield, E. E., Horne, R. B., Glauert, S. A., Menietti, J. D., Shprits, Y. Y., and Kurth, W. S. (2018). Formation of Electron Radiation Belts at Saturn by Z-Mode Wave Acceleration. *Nat. Commun.* 9, 5062. doi:10.1038/s41467-018-07549-4

Woodfield, E. E., Horne, R. B., Glauert, S. A., Menietti, J. D., and Shprits, Y. Y. (2014). The Origin of Jupiter's Outer Radiation Belt. *J. Geophys. Res. (Space Phys.* 119, 3490. doi:10.1002/2014JA019891

Xiang, Z., Li, X., Kapali, S., Gannon, J., Ni, B., Zhao, H., et al. (2021). Modeling the Dynamics of Radiation Belt Electrons with Source and Loss Driven by the Solar Wind. *J. Geophys. Res. Space Phys.* 126, e2020JA028988. doi:10.1029/2020JA028988

Xiang, Z., Tu, W., Li, X., Ni, B., Morley, S. K., and Baker, D. N. (2017). Understanding the Mechanisms of Radiation Belt Dropouts Observed by Van Allen Probes. *J. Geophys. Res. Space Phys.* 122, 9858–9879. doi:10.1002/2017JA024487

Yuan, C.-J., Roussos, E., Wei, Y., Krupp, N., Sun, Y. X., and Hao, Y. X. (2021). Cassini Observation of Relativistic Electron Butterfly Distributions in Saturn's Inner Radiation Belts: Evidence for Acceleration by Local Processes. *Geophys. Res. Lett.* 48, e92690. doi:10.1029/2021GL092690

Yuan, C.-J., Roussos, E., Wei, Y., and Krupp, N. (2020). Sustaining Saturn's Electron Radiation Belts through Episodic, Global-Scale Relativistic Electron Flux Enhancements. *J. Geophys. Res. (Space Phys.* 125, e27621. doi:10.1029/2019JA027621

Yuan, C., Zuo, Y., Roussos, E., Wei, Y., Hao, Y., Sun, Y., et al. (2021). Large-scale Episodic Enhancements of Relativistic Electron Intensities in Jupiter's Radiation Belt. *Earth Planet. Phys.* 5, 314. doi:10.26464/epp2021037

Zhang, X.-J., Mourenas, D., Artemyev, A. V., Angelopoulos, V., Bortnik, J., Thorne, R. M., et al. (2019). Nonlinear Electron Interactionwith Intense Chorus Waves: Statisticsof Occurrence Rates. *Geophys. Lett.* 46, 7182–7190. doi:10.1029/2019GL083833

Zhao, H., Baker, D. N., Jaynes, A. N., Li, X., Elkington, S. R., Kanekal, S. G., et al. (2017). On the Relation between Radiation Belt Electrons and Solar Wind Parameters/geomagnetic Indices: Dependence on the First Adiabatic Invariant and L. *J. Geophys. Res. Space Phys.* 122, 1624–1642. doi:10.1002/2016JA023658

Zhao, H., Baker, D. N., Li, X., Jaynes, A. N., and Kanekal, S. G. (2018). The Acceleration of Ultrarelativistic Electrons during a Small to Moderate Storm of 21 April 2017. *Geophys. Res. Lett.* 45. doi:10.1029/2018GL078582

Zhao, H., Baker, D. N., Li, X., Jaynes, A. N., and Kanekal, S. G. (2019a). The Effects of Geomagnetic Storms and Solar Wind Conditions on the Ultrarelativistic Electron Flux Enhancements. *J. Geophys. Res. Space Phys.* 124, 1948–1965. doi:10.1029/2018JA026257

Zhao, H., Baker, D. N., Li, X., Malaspina, D. M., Jaynes, A. N., and Kanekal, S. G. (2019b). On the Acceleration Mechanism of Ultrarelativistic Electrons in the Center of the Outer Radiation Belt: A Statistical Study. *J. Geophys. Res. Space Phys.* 124, 8590–8599. doi:10.1029/2019JA027111

Zhao, H., Johnston, W. R., Baker, D. N., Li, X., Ni, B., Jaynes, A. N., et al. (2019c). Characterization and Evolution of Radiation Belt Electron Energy Spectra Based on the Van Allen Probes Measurements. *J. Geophys. Res. Space Phys.* 124, 4217–4232. doi:10.1029/2019JA026697

Zhao, H., Li, X., Baker, D. N., Claudepierre, S. G., Fennell, J. F., Blake, J. B., et al. (2016). Ring Current Electron Dynamics during Geomagnetic Storms Based on the Van Allen Probes Measurements. *J. Geophys. Res. Space Phys.* 121, 3333–3346. doi:10.1002/2016JA022358

Zhao, H., Sarris, T. E., Li, X., Weiner, M., Huckabee, I. G., Baker, D. N., et al. (2021). Van Allen Probes Observations of Multi-MeV Electron Drift-Periodic Flux Oscillations in Earth's Outer Radiation Belt during the March 2017 Event. *J. Geophys. Res. Space Phys.* 126, e2021JA029284. doi:10.1029/2021JA029284

Zheng, L., Chan, A. A., O'Brien, T. P., Tu, W., Cunningham, G. S., Albert, J. M., et al. (2016). Effects of Magnetic Drift Shell Splitting on Electron Diffusion in the Radiation Belts. *J. Geophys. Res. Space Phys.* 121 (11), 985–12,000. doi:10.1002/2016JA023438

Zong, Q.-G., Zhou, X.-Z., Wang, Y. F., Li, X., Song, P., Baker, D. N., et al. (2009). Energetic Electron Response to ULF Waves Induced by Interplanetary Shocks in the Outer Radiation Belt. *J. Geophys. Res.* 114, A10204. doi:10.1029/2009JA014393

Zong, Q. (2022). Magnetospheric Response to Solar Wind Forcing: Ultra-low-frequency Wave–Particle Interaction Perspective. *Ann. Geophys.* 40, 121–150. doi:10.5194/angeo-40-121-2022

Zong, Q., Rankin, R., and Zhou, X. (2017). The Interaction of Ultra-low-frequency Pc3-5 Waves with Charged Particles in Earth's Magnetosphere. *Rev. Mod. Plasma Phys.* 1, 10. doi:10.1007/s41614-017-0011-4

Conflict of Interest: The authors declare that the research was conducted in the absence of any commercial or financial relationships that could be construed as a potential conflict of interest.

Publisher's Note: All claims expressed in this article are solely those of the authors and do not necessarily represent those of their affiliated organizations, or those of the publisher, the editors and the reviewers. Any product that may be evaluated in this article, or claim that may be made by its manufacturer, is not guaranteed or endorsed by the publisher.